Table 1. Gene expression profiles in brains of MyD88- and TRIF-deficient mice on day 6 after PbA infection

WT (B6)[a]	MyD88$^{-/-a}$	WT (B6.129)[a]	TRIF$^{-/-a}$	Gene product (symbol)	GenBank accession number
Genes that require solely MyD88 (MyD88 dependent)[b]					
280	49	155	91	*Membrane-spanning 4-domains, subfamily A, member 4B (Ms4a4b)*	BB199001
250	70	75	101	*Granzyme B (Gzmb)*	NM_013542.1
80	5	70	333	*Lipocalin 2 (24p3)*	X14607.1
60	0.5	23.75	22	*Small inducible cytokine A3 (Scya3) (CCL3; MIP 1α)*	NM_011337.1
55.4	7.9	15.2	71	*Schlafen 1 (Slfn1)*	NM_011407.1
44	2.6	58	50	*ESTs*	BB239429
40	15	4.1	20.2	*Activating transcription factor 3 (Atf3)*	BC019946.1
38	5.3	25.8	40.7	*Interferon-induced protein with tetratricopeptide repeats 1 (Ifit1)*	NM_008331.1
37.4	2.3	6.7	5.4	*Leucine-rich alpha-2-glycoprotein (Lrg-pending)*	NM_029796.1
36	1.9	15	16	*Haptoglobin (Hp)*	NM_017370.1
34.7	7.7	21.7	26	*Viral hemorrhagic septicemia virus (VHSV)-induced gene 1 (Vig1)*	NM_021384.1
30.8	4.7	45	25	*2-5 oligoadenylate synthetase-like 2 (Oasl2)*	BQ033138
30.2	3.7	22.6	13.7	*transporter 1, ATP-binding cassette, sub-family B (MDR/TAP* also called *Tap-1)*	BC024897.1
28.4	7	18.6	10.5	*Programmed cell death 1 ligand 1 (Pdcd1l1-pending)*	NM_021893.1
28	4.5	16.6	14.4	*Interferon-induced protein 44 (Ifi44)*	NM_133871.1
25.8	1	52	35.7	*Kallikrein 7 (Klk7)*	NM_011872.1
25.3	1.9	6.2	4.7	*Eukaryotic translation initiation factor 2-alpha kinase 2 (Eif2ak2)*	AV328340
24.8	3.7	19	17	*Interferon-stimulated protein* (15 kDa) *(Isg15)*	AK019325.1
24.2	3.5	15	27.7	*ESTs*	BB132493
23.9	4.6	28	17.8	28-kDa *interferon alpha responsive protein (5830458K16Rik)*	NM_023386.1
22.4	0.7	7.2	8.4	*Interleukin 1 receptor, type II (Il1r2)*	NM_010555.1
21.1	7.8	22.4	35.7	*Ubiquitin-specific protease 18 (Usp18)*	NM_011909.1
20.2	1.7	5.3	13.6	*Plasma membrane-associated protein, S3-12 (S3-12-pending)*	NM_020568.1
19	6.7	11.3	7.6	*Guanylate nucleotide-binding protein 3 (Gbp3)*	NM_018734.1
17.2	3.5	25	10.5	*Interferon-inducible protein 1 (Ifi1* also called *LRG-47)*	NM_008326.1
17.1	2.7	12	10.4	*Fc fragment of IgG, low affinity IIIa, receptor*	BC027310.1
17	4.5	15.7	19	*Interferon-induced protein with tetratricopeptide repeats 3 (Ifit3)*	NM_010501.1
16.5	4	13.4	13	*Interferon regulatory factor 7 (Irf7)*	NM_016850.1
16	1.8	4.8	6.65	*Formyl peptide receptor, related sequence 2 (Fpr-rs2* also called *Fpr-2)*	NM_008039.1
15.8	2.2	7.5	14.2	*Histocompatibility 2, class II antigen A, beta 1 (H2-Bf)*	M15848.1
15.7	2.5	11.7	16.4	*Membrane-spanning 4-domains, subfamily A, member 9 (Ms4a9* also called *Ms4a4c)*	NM_022429.1
15.6	2.1	14	17	*Histocompatibility 2, complement component factor B (H2-Bf)*	NM_008198.1
14.8	3.5	12.4	12.6	*Peptidylprolyl isomerase C-associated protein (Ppicap* also called *CyCAP)*	NM_011150.1
14.4	2	12	12	*Cyclin-dependent kinase inhibitor 1A (P21) (Cdkn1a)*	NM_007669.1
13.4	2.4	14.7	8	*Interferon-induced protein 35 (Ifi35)*	AW986054
11.3	2.3	10.9	5.6	*Histocompatibility 2, T region locus 23 (H2-T23)*	NM_010398.1
11.3	0.8	5.5	3	*Chemokine (C-C) receptor 1 (Cmkbr1)*	BC011092.1
11.2	1.5	12.1	10.2	*Schlafen 2 (Slfn2)*	NM_011408.1
11	0.8	5	4	*S100 calcium-binding protein A8 (calgranulin A) (S100a8)*	NM_013650.1
11	1.3	2.5	2.2	*Glucocorticoid-regulated inflammatory prostaglandin synthase (griPGHS)*	M88242.1
10.2	2.4	7.1	6.3	*Complement component 4 (C4)*	NM_009780.1
10.1	2.3	10.3	10.6	*Signal transducer and activator of transcription 1 (Stat1)*	BM239586
10	3.9	5.5	4	*Fibrinogenangiopoietin-related protein (Angptl4)*	NM_020581.1
9.8	0.8	3.8	2.2	*CD14 antigen (Cd14)*	NM_009841.1
9.5	2	4.6	8.8	*F-box protein 39 (Fbxo39)*	BB645745
9.2	1.2	8.8	4.8	*Apolipoprotein D (Apod)*	AV332635
9	2.75	14	8.3	*Tripartite motif protein 30 (Trim30Rpt1)*	BM240719

Table continues

Table 1. Continued

WT (B6)[a]	MyD88$^{-/-a}$	WT (B6.129)[a]	TRIF$^{-/-a}$	Gene product (symbol)	GenBank accession number
8.7	2	7	7.4	*Paired-Ig-like receptor A6* (*Pira6*)	NM_011093.1
8.6	0.8	2.2	1.2	*Thrombospondin 1* (*THBS1*)	AV026492
8.3	2.5	7.5	9.2	*Lectin, galactose-binding, soluble 9* (*Lgals9*)	NM_010708.1
8.3	3.6	4	3.5	*Interferon concensus sequence-binding protein* (*Icsbp*)	BG069095
8	2.4	22.3	21.8	*Similar to interferon activated gene 203*	BM241008
7.5	1.4	7.4	4.8	*Integrin beta 2* (*Itgb2*)	NM_008404.1
7.3	0.8	6.3	4.6	*Cathepsin C* (*Ctsc*)	NM_009982.1
7.1	2.2	8.8	8.1	*Interferon-dependent positive acting transcription factor 3 gamma* (*Isgf3g* also called *Irf9*)	NM_008394.1
7.1	1.7	9.5	7.3	*Serum amyloid A 3* (*SAA3*)	NM_011315.1
6.8	1	3.8	2.7	*Zinc finger protein 36* (*Zfp36* also called *Tis11*)	X14678.1
5.9	2.4	8.5	11.4	*Interferon-induced protein with tetratricopeptide repeats 2* (*Ifit2*)	NM_008332.1
5.85	2.4	11.9	6.4	*Histocompatibility 2, D region locus 1* (*H2-D1*)	NM_010380.1
5.8	1.8	6.2	23	*Mx1 protein* (*Mx1*)	M21039.1
5.5	0.7	5.45	3.5	*FK506-binding protein 5* (51 kDa) (*Fkbp5*)	BC015260.1
5.48	0.9	5	2.6	*Metallothionein 2* (*Mt2*)	AA796766
5.43	1.6	4.28	2.5	*Interferon regulatory factor 1* (*Irf1*)	NM_008390.1
5.3	0.6	3.3	3.4	*Small inducible cytokine A9* (*Scya9*) (*CCL9*)	NM_011338.1
5.2	2.5	6.8	8.3	*Mda5* (*Ifih1* also called *Helicard*)	AY075132.1
5.1	0.6	3.8	2	*CD86 antigen* (*CD86*)	AF065897.1
5	0.6	2.6	2.9	*C-C chemokine receptor 5* (*CCR5*)	D83648.1
3.7	1.4	5	4.75	*Interferon-stimulated protein* (20 kDa) (*Isg20*)	BC022751.1
3.25	1	7	3.6	*Small inducible cytokine A4* (*ScyA4*) (*CCL4* also called *MIP-1β*)	AF128218.1

[a]Fold increase in mRNA expression in PbA-infected brain tissue compared with that in uninfected brain tissue. [b]Genes in which changes were <2-fold between WT and mutant mice were classified as 'independent', whereas those with a >2-fold difference were classified as 'dependent'. A cut-off value was determined as a 5-fold change in the infected brains compared with those in uninfected WT mice.

genes, including those coding for chemokines related to lymphocyte recruitment, and lymphocyte-related genes, some of which have been reported as critical for CM pathogenesis (12), prompted us to examine the role of MyD88 in recruitment of lymphocytes during CM pathogenesis.

MyD88-dependent recruitment of CCR5$^+$, CD8$^+$ T cells and CD11c$^+$ DCs, including B220$^+$, NK1.1$^+$ cells, into PbA-infected mouse brain

It has been shown that recruitment and activation of T cells in the brain during PbA infection play a critical role in CM pathogenesis (37, 38). Based on the brain mRNA expression profile in PbA-infected mice, we examined whether such T cell recruitment occurs and it is controlled by MyD88. Brain cells were isolated from WT or MyD88-deficient mice at 6 days after PbA infection, and analyzed for the number and type of cells by flow cytometry. Similar numbers of mononuclear cells were recovered from all groups of brains (uninfected naive mice contained $14.2 \times 10^6 \pm 4.7 \times 10^6$ cells per brain, WT mice at day 6 of infection contained $14.9 \times 10^6 \pm 8 \times 10^6$ cells per brain and MyD88$^{-/-}$ mice at day 6 of infection contained $10.2 \times 10^6 \pm 1 \times 10^6$ cells per brain, $n = 3$–6 mice per group). Large numbers of Thy1.2$^+$ and TCRβ$^+$ T cells were observed among cells isolated from the brain at 6 days after infection, while almost no T cells were stained in naive brains suggesting negligible contamination of the cells from the blood flow (Fig. 4A). More than 70% of these T cells in the infected WT brain were CD8 positive, and the remainder were CD4 positive (Fig. 4A). These CD8$^+$ T cells infiltrating the brain also expressed CCR5, whose mRNA was up-regulated in DNA microarray analysis (Fig. 4A and Table 1). Of note, CCL3 (also named MIP-1α), the ligand for CCR5, was also highly up-regulated in the infected brain (Fig. 3 and Table 1). In sharp contrast, the brains of MyD88-deficient mice with no CM symptoms had dramatically fewer CCR5$^+$, CD8$^+$ T cells (Fig. 4A). As CCL3 was highly up-regulated in the brain, these results suggest that CCR5$^+$, CD8$^+$ T cells may be recruited to the brain via MyD88-dependent up-regulation of CCL3.

We also found that CD11c$^+$ DCs, but not B220$^+$ B cells, were increased in number in infected brains in a MyD88-dependent manner (Fig. 4B). Among those CD11c$^+$ cells increased, we found that CD11c$^+$ and NK1.1$^+$ cells were also increased in a MyD88-dependent manner, all of which were CD11c$^+$ and B220 dim (Fig. 4B), which displayed identical staining pattern to those identified as hybrid type cells for DCs and NK cells namely IFN-producing killer dendritic cells (IKDCs) (type-I and -II) (28, 29) and certain NK cell subsets as previously described (39, 40). These results suggest that MyD88-mediated signaling triggers expression of genes, such as chemokines, including CCL3, resulting in recruitment of CCR5$^+$, CD8$^+$ T cells, as well as CD11c$^+$ DCs, including CD11c$^+$, B220$^+$ and NK1.1$^+$ cells into the brain. It was also shown by DNA microarray analysis and RT–PCR

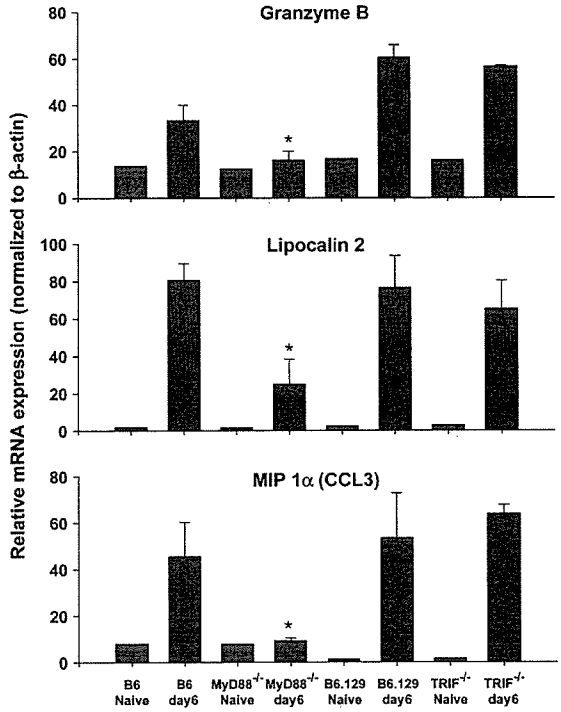

Fig. 3. MyD88-dependent brain mRNA gene expression after PbA infection. MyD88$^{-/-}$ and TRIF$^{-/-}$ mice and their WT controls were infected with 10^6 of PbA iRBCs. Brains were removed 6 days after infection and mRNA expression was analyzed by RT-PCR. Density of the PCR products in ethidium bromide-stained gel was measured by NIH image software. Results (mean ± SD) are presented as relative units normalized to β-actin, which were obtained from three infected mice per group, and experiments were repeated twice. *$P < 0.05$, infected MyD88$^{-/-}$ or TRIF$^{-/-}$ mice versus infected WT mice (Student's *t*-test).

that genes such as *Ms4a4b* (also called *Chandra*), *granzyme B* and *Ifng*, which are expressed in CD4$^+$ and CD8$^+$ T cells and NK1.1$^+$ cells, and possibly in CD11c$^+$, B220$^+$ and NK1.1$^+$ cells (36), were also highly up-regulated in WT mice brains, but not in those from infected MyD88-deficient mice or uninfected mice (Table 1).

Role of TLRs in the pathogenesis of CM

MyD88 is an essential adaptor molecule for intracellular signaling mediated by most TLRs, as well as IL-1R/IL-18R. Previous reports suggest that IL-18 is up-regulated and involved in protective immunity, rather than lethal complications such as CM in PbA infection (9). *Plasmodium* spp. have been shown to contain ligands for TLR2 and TLR9, such as GPI anchor and hemozoin, respectively (16, 17), which prompted us to examine whether these TLRs are, in fact, involved in the pathogenesis of CM. We infected mice deficient for TLR2, TLR4, TLR5, TLR7 or TLR9 with PbA, and then monitored incidence of CM and survival. Each TLR-deficient mouse was backcrossed to C57BL/6 background at least for eight generations. A significant number of mice lacking TLR2 or TLR9, but not TLR4, TLR5 or TLR7, survived CM and early death between 6 and 12 days after infection (Fig. 5A–E) ($P < 0.001$ for WT versus TLR2$^{-/-}$ mice; $P = 0.027$ for WT versus TLR9$^{-/-}$ mice; $P > 0.05$ for WT versus TLR4$^{-/-}$, TLR5$^{-/-}$ or TLR7$^{-/Y}$ mice by log rank survival analysis). Overall escape from CM in TLR2- and TLR9-deficient mice until day 12 after infection was significantly higher [10.55% of WT (B6) mice ($n = 28$) versus 55% of TLR2$^{-/-}$ mice ($n = 21$) escaped from CM; 14.7% of WT (B6) mice ($n = 27$) versus 45.8% of TLR9$^{-/-}$ mice ($n = 19$) escaped from CM]. However, TLR4-, TLR5- or TLR7-deficient mice could not escape from CM [10.55% of WT (B6) mice ($n = 28$) versus 0% 16.75% of TLR4$^{-/-}$ mice ($n = 20$) escaped from CM; 14.28% of WT (B6) mice ($n = 14$) versus 0% of TLR5$^{-/-}$ mice ($n = 11$) escaped from CM; 0% of WT (B6) mice ($n = 5$) versus 0% of TLR7$^{-/Y}$ mice ($n = 5$) escaped from CM].

Of note, parasitemia was comparable between the WT and each strain of TLR-deficient mice (Fig. 5A and B), which survived CM, while that of MyD88$^{-/-}$ was slightly higher (Fig. 1A). It may be due to compensated innate and adaptive immune responses in TLR2$^{-/-}$ or TLR9$^{-/-}$ mice compared with MyD88$^{-/-}$ mice which lack combined effects of each TLR. While we did not formally exclude the less likely involvement of IL-1 and IL-18, which also require MyD88 for their subsequent functions, these results strongly suggest that TLR2 and TLR9, but not TLR4, TLR5 or TLR7, are involved in the pathogenesis of CM, but not in controlling parasitemia during PbA infection.

Systemic responses and hemozoin load in the brain

Based on the evidence that pro-inflammatory cytokines such as IFNγ, IL-12 and TNFα are associated with the severity of malaria infection including CM (7–9), we investigated the role of MyD88/TLR2/TLR9 pathways on the systemic productions of such cytokines in serum at day 6 after infection. Productions of serum cytokines IFNγ, TNFα and IL-12p40 were significantly dependent on MyD88 ($P < 0.05$ by Mann–Whitney *U*-test) (Fig. 6A). The up-regulation of serum IFNγ, TNFα and IL-12p40 was significantly reduced in MyD88-deficient mice, but not in TRIF- or TLR2-deficient mice. On the other hand, in TLR9$^{-/-}$ mice only TNFα production was TLR9 dependently secreted after PbA infection (Fig. 6A, $P < 0.05$, Mann–Whitney *U*-test). These results suggested that PbA infection causes systemic cytokine productions via MyD88-dependent signaling; however, systemic cytokine productions are not critical for CM development.

We also counted hemozoin clusters in brains of TLR2$^{-/-}$ and TLR9$^{-/-}$ mice after Prussian blue staining and found that hemozoin accumulation was significantly reduced in TLR2- and TLR9-deficient mice brains compared with that in WT brains at day 6 (Fig. 6B, $P < 0.038$ and $P < 0.019$, respectively, by Mann–Whitney *U*-test).

Discussion

In this study, we showed, for the first time, that TLRs and their adaptor molecules play distinct roles in CM pathogenesis. Mice deficient in MyD88, but not in TRIF, displayed significantly less CM-characteristic neurological symptoms, which resulted in significantly reduced mortality. This was supported by histological analysis in which the brains from infected

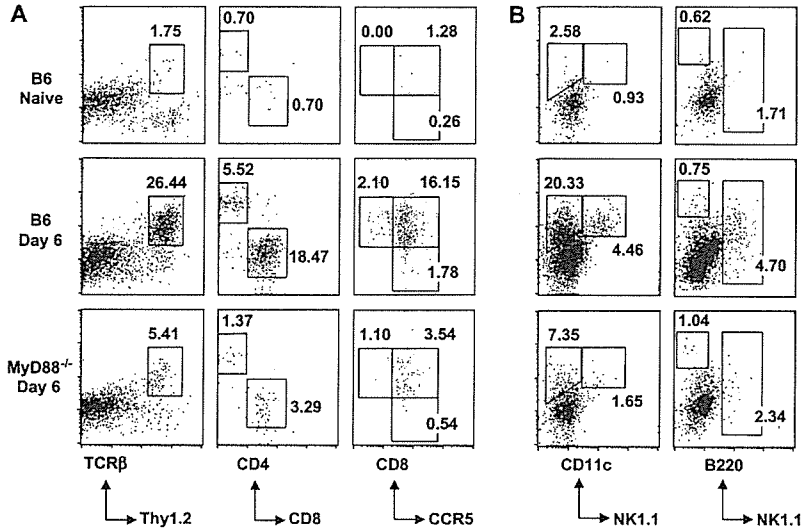

Fig. 4. MyD88-dependent recruitment of CCR5$^+$, CD8$^+$ T cells and CD11c$^+$ cells, including CD11c$^+$, B220$^+$ and NK1.1$^+$ cells, into PbA-infected brain. Brain lymphocytes were isolated from infection-naive or PbA-infected WT or MyD88$^{-/-}$ mice, and stained with labeled antibodies as described in the experimental procedure. (A) Thy1.2$^+$ and TCRβ$^+$ T cells (left panel) were stained with antibodies against CD4, CD8 and/or CCR5 (middle and right panels). (B) Cells were stained with anti-CD11c, NK1.1 and/or B220. Numbers represent the percentage of gated cell population in isolated brain lymphocytes. Results are representative of one mouse from each group of three mice. Experiments were repeated three times with similar results.

MyD88-deficient mice displayed reduced endothelial cell damage and sequestration of infected erythrocytes. We could detect hemozoin in infected WT brain blood vessels, as well as in the other brain tissues by microscopy, which was significantly less in MyD88-deficient mice. Moreover, flow cytometry of the recovered lymphocytes from the infected brain suggested that infiltration of T cells, most of which are CCR5$^+$, CD8$^+$ T cells and CD11c$^+$ DCs, including CD11c$^+$, B220$^+$ and NK1.1 cells, is controlled at least in part by MyD88-dependent signaling. Although not all MyD88-deficient mice survived CM caused by PbA infection, our results strongly suggest that MyD88, but not TRIF, is a key signaling molecule in CM pathogenesis, at least in currently available experimental CM models.

The effect of MyD88 on CM was more obvious in local brain where CM symptom attribute to, rather than systemic control of parasitemia as well as inflammation. Damage of brain blood vessels is a characteristic feature of CM pathogenesis, such as destruction of the endothelial cell layer, sequestration of iRBCs and infiltration of lymphocytes, all of which are dramatically reduced in MyD88-deficient mice compared with either WT or TRIF-deficient mice. We observed parasite sequestration and hemozoin load in these damaged blood vessels in WT infected mice, which was almost diminished in MyD88-deficient mice. Together with the other observation that hemozoin was also detected in brain tissue, and that the microglia cell line was activated by both crude extracts of the iRBCs and hemozoin, but not uninfected RBCs, this suggests that residual microglial cells may be activated by iRBCs that are known to contain TLR ligands, such as GPI and/or hemozoin (16, 17), which have escaped or leaked through the damaged blood–brain barrier.

Comprehensive analysis of MyD88- and/or TRIF-dependent genes in response to PbA infection revealed several important genes that could be involved in CM pathogenesis. MyD88-depedent genes up-regulated by PbA infection included not only those up-regulated by the microglial cell line, but also type-I or -II IFN-inducible genes, T or NK cell-related genes and stress response genes. A recent report identified several genes such as *Gzmb*, *Samhd1*, *Fkbp5*, *Ifit3*, *Igf2r*, *Ctla2a* and *C1qb* which were up-regulated specifically in CM-susceptible mice strains infected with PbA (32). Our results confirmed and further extended these findings; *Gzmb* and *Ifit3* were up-regulated during PbA infection, which was exclusively dependent on MyD88. In addition, we found that *Isg15*, *Mx1*, *Cxcl10* (*IP-10*), *Ccl3* (*MIP-1α*), *Ccr5* and *serum amyloid A* were also up-regulated by PbA infection in a MyD88-dependent manner. Of note, MIP-1α was reported to be up-regulated by hemozoin in macrophages (41). Moreover, *Lipocalin 2* (*24p3*), a gene important for iron metabolism and for resistance against certain bacteria (42) and presumably important marker for severe malaria in humans (35), was highly up-regulated in the brain of PbA-infected mice in a MyD88-dependent manner (Table 1 and Fig. 3). Our preliminary data, however, suggest that mice deficient for *Lipocalin 2* (*24p3*) suffered from and died from CM, as did WT mice (C. Coban, K. J. Ishii, S. Sato and S. Akira, unpublished results).

Among the MyD88-dependent CM-related genes, we noted some that may be involved in innate immune responses (especially type-I and -II IFN-inducible genes) and the recruitment of lymphocytes, such as T cells and/or NK cells. We were initially interested in type-I IFN-inducible genes; however, infection of mice lacking IFNαβR or TBK1 (and/or TNF, which are deficient for TRIF- or TLR-independent type-I IFN

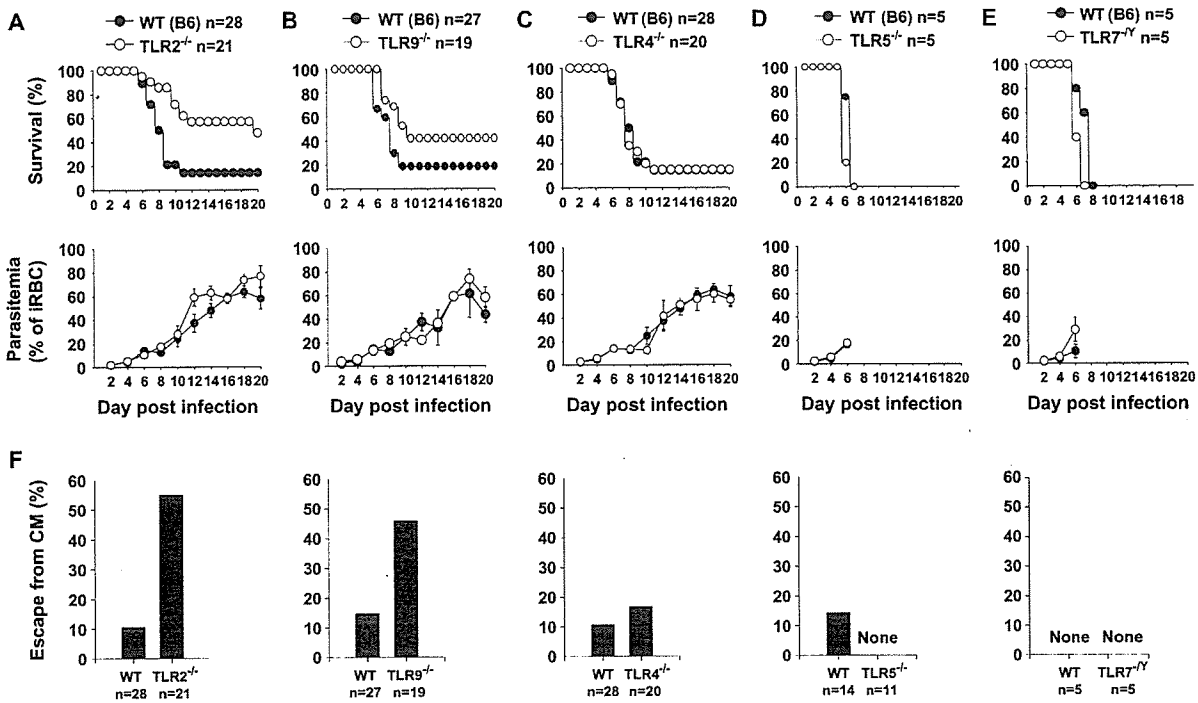

Fig. 5. TLR2$^{-/-}$ and TLR9$^{-/-}$ mice have decreased susceptibility to CM. WT (B6) or mice lacking (A) TLR2, (B) TLR9, (C) TLR4, (D) TLR5 or (E) TLR7 ($n = 28$ for WT and $n = 21$ for TLR2$^{-/-}$, $n = 27$ for WT and $n = 19$ for TLR9$^{-/-}$, $n = 28$ for WT and $n = 20$ for TLR4$^{-/-}$, $n = 5$ for WT and $n = 5$ for TLR5$^{-/-}$ and $n = 5$ for WT and $n = 5$ for TLR7$^{-/Y}$) were infected with 10^6 iRBCs of PbA strain. Survival was monitored daily. Parasitemia was examined from Giemsa-stained blood smears every 2 days (mean parasitemia ± SE). $P < 0.001$ for the percentage survival curve of WT versus TLR2$^{-/-}$ mice, and $P = 0.027$ for that of WT versus TLR9$^{-/-}$ mice by log rank test. (F) Total escape from CM in TLR-deficient mice until day 12 after infection. In all, 10.55% of WT (B6) mice ($n = 28$) escaped from CM versus 55% of TLR2$^{-/-}$ mice ($n = 21$), 14.7% of WT (B6) mice ($n = 27$) escaped from CM versus 45.8% of TLR9$^{-/-}$ mice ($n = 19$), 10.55% of WT (B6) mice ($n = 28$) escaped from CM versus 16.75% of TLR4$^{-/-}$ mice ($n = 20$), 14.28% of WT (B6) mice ($n = 14$) escaped from CM versus none of TLR5$^{-/-}$ mice ($n = 11$) and none of WT (B6) mice ($n = 5$) escaped from CM versus none of TLR7$^{-/Y}$ mice ($n = 5$). 'None' implies that no infected mice could survive.

induction) suffer from CM and died comparably to those of WT mice (C. Coban, K. J. Ishii and S. Akira, unpublished results). Rather, type-II IFNγ may play a more critical role in MyD88-dependent IFN-inducible genes up-regulated during PbA infection, since systemic as well as brain IFNγ but not IFNα were up-regulated in a MyD88-dependent manner (Fig. 6A, and data not shown). In fact, systemic production of IFNγ, TNFα and IL-12p40 was MyD88 dependent, but not TRIF dependent (Fig. 6A). In case of mice lacking TLR2 or TLR9, however, systemic cytokines were not altered except TNFα in TLR9-deficient mice (Fig. 6A), suggesting that systemic cytokines such as IFNγ were compensated between TLR2 and TLR9, although mice lacking TLR2 or TLR9 survived CM significantly better than WT (Fig. 5). It is also conceivable that the systemic cytokine production such as IFNγ may be regulated by TLR-independent, MyD88-dependent signaling pathway, in which IL-1R and IL-18R utilize. We then focused on genes related to T and NK cells which may be the result of their migration into brain controlled by chemokine genes such as *Ccl3*, *Ccl9* and *Ccr5* which were up-regulated in a MyD88-dependent manner (Table 1 and Fig. 3). In fact, we found that both CD4$^+$ and CCR5$^+$, CD8$^+$ T cells and CD11c$^+$ DCs including CD11c$^+$, B220$^+$ and NK1.1$^+$ cells infiltrated into the brain after PbA infection, which was clearly MyD88 dependent. The cells positive for CD11c, B220 and NK1.1 were with identical staining pattern of newly described IKDCs (28, 29) and certain subsets of NK cells expressing either CD11c or B220 (39, 40), suggesting that they may possess cytotoxic ability via *granzyme*. In addition, we found that certain chemokines were highly up-regulated in a MyD88-dependent manner; CCL3 and CCL4 are known to recruit CCR5-positive cells, including T cells, macrophages and DCs. In agreement with previous reports showing that perforin-deficient C57Bl/6 mice (11, 43, 44) and CCR5-deficient mice (12) which lack their killing and recruiting functions, respectively, display increased resistance to CM, we conclude that the MyD88-dependent recruitment of T cells, DCs and cells expressing both DC and NK markers, possibly via chemokine productions in the brain, may play a critical role in CM pathogenesis.

Results obtained in similar experiments using various TLR-deficient mice suggest that TLR2- and/or TLR9-mediated, MyD88-dependent innate immune cascades may play a critical role in the pathogenesis of CM. This coincides with recent evidence that GPI and hemozoin are found to be agonists for TLR2 and TLR9, respectively (16, 17). TLR2 and TLR9 have been shown to co-operate for protective immune responses

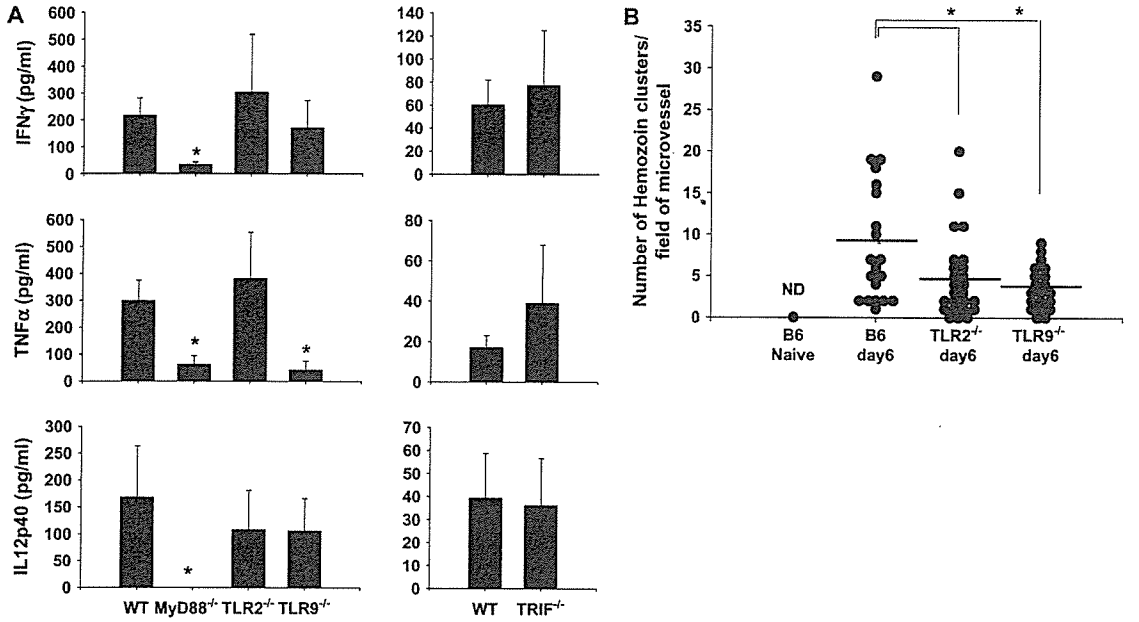

Fig. 6. Systemic cytokine responses and brain hemozoin load after PbA infection. (A) MyD88$^{-/-}$, TRIF$^{-/-}$, TLR2$^{-/-}$ and TLR9$^{-/-}$ mice and their WT controls were infected with 10^6 of PbA iRBCs. Serum levels of IFNγ, TNFα and IL-12p40 at day 6 after infection with PbA were measured by ELISA. Results (mean ± SE) are from three different experiments that cytokine levels were measured at the same time (n = 10–25 mice per group). *P = 0.02 for IFNγ of MyD88$^{-/-}$ versus WT mice, *P = 0.005 for TNFα of MyD88$^{-/-}$ versus WT mice *P = 0.002 for TLR9$^{-/-}$ versus WT mice and *P < 0.001 for IL-12p40 of MyD88$^{-/-}$ versus WT mice (Mann–Whitney U-test). (B) Brain tissue sections were stained with Prussian blue, and hemozoin clusters in infiltrated brain vessels were counted in 20–25 microscopic fields by light microscopy. TLR2$^{-/-}$ and TLR9$^{-/-}$mouse brains had significantly lower numbers of hemozoin clusters in each area counted (P < 0.038 and P < 0.019, respectively, Mann–Whitney U-test, n = 2 or 3 per group). ND represents not detected in uninfected naive mice.

against various infectious organisms including *Mycobacterium tuberculosis* (45), while TLR9 and TLR2 have been shown to play a reciprocal role in protective immunity and pathology during *Herpes simplex virus* infection, respectively (46). In the case of PbA infection, an absence of TLR2 or TLR9 increases resistance to CM-related mortality but not parasitemia, suggesting that these two TLRs play a critical role in the pathogenesis, and not in protective immunity. A similar strategy was observed for West Nile Virus to utilize TLR3 to facilitate infection in the brain (47). However, further investigation may be needed to clarify whether these TLRs play similar roles in the case of the other *Plasmodium* species such as *Plasmodium yoelii* or *chabaudi*.

In contrast to TLR2 and TLR9, the other TLRs utilizing MyD88 as an essential adaptor, such as TLR5 and TLR7, as well as TLR4, which utilize both MyD88 and TRIF, were not involved in CM pathogenesis and its resultant mortality (Fig. 5). It is of note that, although TRIF-deficient mice die in the same way as WT mice, some genes up-regulated by PbA infection were TRIF dependent (Supplementary Table 2, available at *International Immunology* Online). These results suggest that there are TRIF-dependent innate immune responses during PbA infection, and therefore, it is interesting to investigate the role of TRIF-dependent recognition in the immune response to PbA infection and to identify as yet unknown ligands. Receptors for IL-1 and IL-18 are also known to utilize MyD88 for their sequential signaling; however, previous reports have suggested that both IL-1 and IL-18 are not involved in CM pathogenesis (8, 9). While specific cell types, by which TLR2 and/or TLR9 mediate MyD88-dependent innate and adaptive immune cascades leading to CM, have not been formally identified, the present study will hopefully help in discerning the complex role of innate immunity in CM pathogenesis.

Overall, the results presented in the current work suggest that innate immune responses via TLR2-, TLR9- and MyD88-dependent pathway are critically involved in the pathogenesis of CM, in which local rather than systemic pro-inflammatory responses plus adaptive immune responses particularly in brain tissue lead to infiltration of CD8 T cells, DCs including those with NK cell marker into brain, and up-regulation of variety of genes related to CM, resulting in the pathogenic changes as we described above. A few information are available whether TLRs or their signaling pathways are involved in human malaria infection; TLR4 frequent single-nucleotide polymorphism (SNP), Asp299Gly, is associated with severe malaria and risk of maternal malaria, whereas TLR9 SNP, T-1486C increased the risk of maternal malaria, but was not associated with severe malaria (48, 49). Although relevance of murine experimental CM models to human CM is under debate; however, our findings with the best available model of CM with PbA infection strongly suggest that host innate immune system against malaria and its exploitation by parasites hold a key to further understanding of pathogenesis of human CM.

Supplementary data

Supplementary figure 1 and tables 1 and 2 are available at *International Immunology* Online.

Acknowledgements

We thank Yukiko Fujita for her excellent technical assistance. This study was supported by grants from the Ministry of Education, Culture, Sports, Science and Technology in Japan and from the 21st Century Center of Excellence Program of Japan.

Abbreviations

APC	allophycocyanin
CM	cerebral malaria
DC	dendritic cell
FBS	fetal bovine serum
GPI	glycosyl-phosphatidylinositol
HE	hematoxylin and eosin
IKDC	IFN-producing killer dendritic cell
iRBC	infected RBC
MyD88	myeloid differentiation primary response gene 88
PbA	*Plasmodium berghei* ANKA
RT	reverse transcription
SNP	single-nucleotide polymorphism
TLR	Toll-like receptor
TNF	tumor necrosis factor
TRIF	TIR domain containing adaptor-inducing IFN-beta
WT	wild type

References

1 Aikawa, M. 1988. Human cerebral malaria. *Am. J. Trop. Med. Hyg.* 39:3.
2 Miller, L. H., Baruch, D. I., Marsh, K. and Doumbo, O. K. 2002. The pathogenic basis of malaria. *Nature* 415:673.
3 Idro, R., Jenkins, N. E. and Newton, C. R. 2005. Pathogenesis, clinical features, and neurological outcome of cerebral malaria. *Lancet Neurol.* 4:827.
4 Good, M. F., Xu, H., Wykes, M. and Engwerda, C. R. 2005. Development and regulation of cell-mediated immune responses to the blood stages of malaria: implications for vaccine research. *Annu. Rev. Immunol.* 23:69.
5 Schofield, L. and Grau, G. E. 2005. Immunological processes in malaria pathogenesis. *Nat. Rev. Immunol.* 5:722.
6 Engwerda, C., Belnoue, E., Gruner, A. C. and Renia, L. 2005. Experimental models of cerebral malaria. *Curr. Top. Microbiol. Immunol.* 297:103.
7 Hunt, N. H. and Grau, G. E. 2003. Cytokines: accelerators and brakes in the pathogenesis of cerebral malaria. *Trends Immunol.* 24:491.
8 Curfs, J. H., van der Meer, J. W., Sauerwein, R. W. and Eling, W. M. 1990. Low dosages of interleukin 1 protect mice against lethal cerebral malaria. *J. Exp. Med.* 172:1287.
9 Singh, R. P., Kashiwamura, S., Rao, P., Okamura, H., Mukherjee, A. and Chauhan, V. S. 2002. The role of IL-18 in blood-stage immunity against murine malaria *Plasmodium yoelii* 265 and *Plasmodium berghei* ANKA. *J. Immunol.* 168:4674.
10 Hansen, D. S., Siomos, M. A., Buckingham, L., Scalzo, A. A. and Schofield, L. 2003. Regulation of murine cerebral malaria pathogenesis by CD1d-restricted NKT cells and the natural killer complex. *Immunity* 18:391.
11 Belnoue, E., Kayibanda, M., Vigario, A. M. *et al.* 2002. On the pathogenic role of brain-sequestered alphabeta CD8+ T cells in experimental cerebral malaria. *J. Immunol.* 169:6369.
12 Belnoue, E., Kayibanda, M., Deschemin, J. C. *et al.* 2003. CCR5 deficiency decreases susceptibility to experimental cerebral malaria. *Blood* 101:4253.
13 Akira, S., Uematsu, S. and Takeuchi, O. 2006. Pathogen recognition and innate immunity. *Cell* 124:783.
14 Ishii, K. J., Coban, C. and Akira, S. 2005. Manifold mechanisms of toll-like receptor-ligand recognition. *J. Clin. Immunol.* 25:511.
15 Adachi, K., Tsutsui, H., Kashiwamura, S. *et al.* 2001. *Plasmodium berghei* infection in mice induces liver injury by an IL-12- and toll-like receptor/myeloid differentiation factor 88-dependent mechanism. *J. Immunol.* 167:5928.
16 Krishnegowda, G., Hajjar, A. M., Zhu, J. *et al.* 2005. Induction of proinflammatory responses in macrophages by the glycosylphosphatidylinositols of *Plasmodium falciparum*: cell signaling receptors, glycosylphosphatidylinositol (GPI) structural requirement, and regulation of GPI activity. *J. Biol. Chem.* 280:8606.
17 Coban, C., Ishii, K. J., Kawai, T. *et al.* 2005. Toll-like receptor 9 mediates innate immune activation by the malaria pigment hemozoin. *J. Exp. Med.* 201:19.
18 Pichyangkul, S., Yongvanitchit, K., Kum-arb, U. *et al.* 2004. Malaria blood stage parasites activate human plasmacytoid dendritic cells and murine dendritic cells through a Toll-like receptor 9-dependent pathway. *J. Immunol.* 172:4926.
19 Adachi, O., Kawai, T., Takeda, K. *et al.* 1998. Targeted disruption of the MyD88 gene results in loss of IL-1- and IL-18-mediated function. *Immunity* 9:143.
20 Yamamoto, M., Sato, S., Hemmi, H. *et al.* 2003. Role of adaptor TRIF in the MyD88-independent toll-like receptor signaling pathway. *Science* 301:640.
21 Takeuchi, O., Hoshino, K., Kawai, T. *et al.* 1999. Differential roles of TLR2 and TLR4 in recognition of gram-negative and gram-positive bacterial cell wall components. *Immunity* 11:443.
22 Hoshino, K., Takeuchi, O., Kawai, T. *et al.* 1999. Cutting edge: Toll-like receptor 4 (TLR4)-deficient mice are hyporesponsive to lipopolysaccharide: evidence for TLR4 as the Lps gene product. *J. Immunol.* 162:3749.
23 Hemmi, H., Kaisho, T., Takeuchi, O. *et al.* 2002. Small anti-viral compounds activate immune cells via the TLR7 MyD88-dependent signaling pathway. *Nat. Immunol.* 3:196.
24 Hemmi, H., Takeuchi, O., Kawai, T. *et al.* 2000. A Toll-like receptor recognizes bacterial DNA. *Nature* 408:740.
25 Uematsu, S., Jang, M. H., Chevrier, N. *et al.* 2006. Detection of pathogenic intestinal bacteria by Toll-like receptor 5 on intestinal CD11c(+) lamina propria cells. *Nat. Immunol.* 7:868.
26 Takeshita, S., Takeshita, F., Haddad, D. E., Janabi, N. and Klinman, D. M. 2001. Activation of microglia and astrocytes by CpG oligodeoxynucleotides. *Neuroreport* 12:3029.
27 Omer, F. M., De Souza, J. B., Corran, P. H., Sultan, A. A. and Riley, E. M. 2003. Activation of transforming growth factor beta by malaria parasite-derived metalloproteinases and a thrombospondin-like molecule. *J. Exp. Med.* 198:1817.
28 Chan, C. W., Crafton, E., Fan, H. N. *et al.* 2006. Interferon-producing killer dendritic cells provide a link between innate and adaptive immunity. *Nat. Med.* 12:207.
29 Taieb, J., Chaput, N., Menard, C. *et al.* 2006. A novel dendritic cell subset involved in tumor immunosurveillance. *Nat. Med.* 12:214.
30 Ishii, K. J., Coban, C., Kato, H. *et al.* 2006. A Toll-like receptor-independent antiviral response induced by double-stranded B-form DNA. *Nat. Immunol.* 7:40.
31 Akira, S. and Takeda, K. 2004. Toll-like receptor signalling. *Nat. Rev. Immunol.* 4:499.
32 Delahaye, N. F., Coltel, N., Puthier, D. *et al.* 2006. Gene-expression profiling discriminates between cerebral malaria (CM)-susceptible mice and CM-resistant mice. *J. Infect. Dis.* 193:312.
33 Medana, I. M., Hunt, N. H. and Chan-Ling, T. 1997. Early activation of microglia in the pathogenesis of fatal murine cerebral malaria. *Glia* 19:91.
34 Dalpke, A. H., Schafer, M. K., Frey, M. *et al.* 2002. Immunostimulatory CpG-DNA activates murine microglia. *J. Immunol.* 168: 4854.
35 Mohammed, A. O., Elghazali, G., Mohammed, H. B. *et al.* 2003. Human neutrophil lipocalin: a specific marker for neutrophil activation in severe *Plasmodium falciparum* malaria. *Acta Trop* 87:279.
36 Xu, H., Williams, M. S. and Spain, L. M. 2006. Patterns of expression, membrane localization, and effects of ectopic expression suggest a function for MS4a4B, a CD20 homolog in Th1 T cells. *Blood* 107:2400.

37 Finley, R. W., Mackey, L. J. and Lambert, P. H. 1982. Virulent *P. berghei* malaria: prolonged survival and decreased cerebral pathology in cell-dependent nude mice. *J. Immunol.* 129:2213.
38 Bauer, P. R., Van Der Heyde, H. C., Sun, G., Specian, R. D. and Granger, D. N. 2002. Regulation of endothelial cell adhesion molecule expression in an experimental model of cerebral malaria. *Microcirculation* 9:463.
39 Laouar, Y., Sutterwala, F. S., Gorelik, L. and Flavell, R. A. 2005. Transforming growth factor-beta controls T helper type 1 cell development through regulation of natural killer cell interferon-gamma. *Nat. Immunol.* 6:600.
40 Hayakawa, Y. and Smyth, M. J. 2006. CD27 dissects mature NK cells into two subsets with distinct responsiveness and migratory capacity. *J. Immunol.* 176:1517.
41 Jaramillo, M., Godbout, M. and Olivier, M. 2005. Hemozoin induces macrophage chemokine expression through oxidative stress-dependent and -independent mechanisms. *J. Immunol.* 174:475.
42 Flo, T. H., Smith, K. D., Sato, S. *et al.* 2004. Lipocalin 2 mediates an innate immune response to bacterial infection by sequestrating iron. *Nature* 432:917.
43 Nitcheu, J., Bonduelle, O., Combadiere, C. *et al.* 2003. Perforin-independent brain-infiltrating cytotoxic CD8+ T lymphocytes mediate experimental cerebral malaria pathogenesis. *J. Immunol.* 170:2221.
44 Potter, S., Chan-Ling, T., Ball, H. J. *et al.* 2006. Perforin mediated apoptosis of cerebral microvascular endothelial cells during experimental cerebral malaria. *Int. J. Parasitol.* 36:485.
45 Bafica, A., Scanga, C. A., Feng, C. G., Leifer, C., Cheever, A. and Sher, A. 2005. TLR9 regulates Th1 responses and cooperates with TLR2 in mediating optimal resistance to *Mycobacterium tuberculosis*. *J. Exp. Med.* 202:1715.
46 Morrison, L. A. 2004. The Toll of herpes simplex virus infection. *Trends Microbiol.* 12:353.
47 Wang, T., Town, T., Alexopoulou, L., Anderson, J. F., Fikrig, E. and Flavell, R. A. 2004. Toll-like receptor 3 mediates West Nile virus entry into the brain causing lethal encephalitis. *Nat. Med.* 10:1366.
48 Mockenhaupt, F. P., Cramer, J. P., Hamann, L. *et al.* 2006. Toll-like receptor (TLR) polymorphisms in African children: common TLR-4 variants predispose to severe malaria. *Proc. Natl Acad. Sci. USA* 103:177.
49 Mockenhaupt, F. P., Hamann, L., von Gaertner, C. *et al.* 2006. Common polymorphisms of toll-like receptors 4 and 9 are associated with the clinical manifestation of malaria during pregnancy. *J. Infect. Dis.* 194:184.

Intraerythrocytic *Plasmodium falciparum* utilize a broad range of serum-derived fatty acids with limited modification for their growth

F. MI-ICHI[1,2], K. KITA[2] *and* T. MITAMURA[1]*

[1] *Department of Molecular Protozoology, Research Institute for Microbial Diseases, Osaka University, 3-1 Yamadaoka, Suita, Osaka 565-0871, Japan*
[2] *Department of Biomedical Chemistry, Graduate School of Medicine, University of Tokyo, 7-3-1 Hongo, Bunkyou-ku, Tokyo 113-0033, Japan*

(*Received 15 March 2006; revised 19 April 2006; accepted 20 April 2006; first published online 19 June 2006*)

SUMMARY

Plasmodium falciparum causes the most severe form of malaria. Utilization of fatty acids in serum is thought to be necessary for survival of this parasite in erythrocytes, and thus characterization of the parasite fatty acid metabolism is important in developing a new strategy for controlling malaria. Here, we examined which combinations of fatty acids present in human serum support the continuous culture of *P. falciparum* in serum-free medium. Metabolic labelling and gas chromatography analyses revealed that, despite the need for particular fatty acids for the growth of intraerythrocytic *P. falciparum*, it can metabolize a broad range of serum-derived fatty acids into the major lipid species of their membranes and lipid bodies. In addition, these analyses showed that the parasite's overall fatty acid composition reflects that of the medium, although the parasite has a limited capacity to desaturate and elongate serum-derived fatty acids. These results indicate that the *Plasmodium* parasite is distinct from most cells, which maintain their fatty acid composition by coordinating *de novo* biosynthesis, scavenging, and modification (desaturation and elongation).

Key words: malaria, desaturase, elongase, lipid metabolism, *Plasmodium falciparum*, fatty acid.

INTRODUCTION

Plasmodium falciparum causes the most severe form of malaria, afflicting people in endemic areas with a very high rate of morbidity and mortality. The clinical symptoms and pathogenesis of this disease are exclusively associated with the asexual multiplication of this parasite in erythrocytes. This parasite requires human serum for its intraerythrocytic proliferation (Trager and Jensen, 1976). Thorough investigation of the essential factors in human serum and their metabolism in the parasite is essential for identifying pathways critical for its growth and, therefore, identification of novel approaches to the treatment of malaria.

Previous studies on serum components that support the intraerythrocytic development of *P. falciparum in vitro* have identified several factors, including high and low density lipoproteins (Grellier *et al.* 1991), long-chain saturated and unsaturated fatty acids in association with BSA (Ofulla *et al.* 1993), and a mixture of lysophosphatidylcholines in association with BSA (Asahi *et al.* 2005); however, studies of fractioned human serum have not been completed. Recently, by fractionating and reducing the components in human serum, we identified palmitic ($C_{16:0}$) and oleic ($C_{18:1,\ n\text{-}9}$) acids in association with lipid-free BSA as a minimal component necessary for complete cell cycle progression and intraerythrocytic development of *P. falciparum in vitro* (Mitamura *et al.* 2000). Indeed, these essential fatty acids have been shown to be metabolized into various lipid species, such as phosphatidylcholine, phosphatidylethanolamine, diacylglycerol, and triacylglycerol, all of which are major constituents of membranes and lipid bodies in the parasite (Vial *et al.* 1982; Palacpac *et al.* 2004).

Several lines of evidence suggest that intraerythrocytic *P. falciparum* has the capacity to generate middle-chain ($C_{10:0}$, $C_{12:0}$, and $C_{14:0}$) but not long-chain fatty acids ($C_{16:0}$ and $C_{18:0}$) through a *de novo* biosynthetic pathway and that this pathway is essential for parasite growth (Surolia and Surolia, 2001). Nevertheless, intraerythrocytic proliferation largely relies on fatty acids derived from human serum; basal medium lacking these fatty acids does not support growth (Mitamura *et al.* 2000). This agrees with the idea that serum-derived long-chain saturated and unsaturated fatty acids are necessary for parasite growth and that scavenging fatty acids

* Corresponding author: Department of Molecular Protozoology, Research Institute for Microbial Diseases, Osaka University, 3-1 Yamadaoka, Suita, Osaka 565-0871, Japan. Tel: +81 6 6879 8279. Fax: +81 6 6879 8281. E-mail: mitamura@biken.osaka-u.ac.jp

Parasitology (2006), **133**, 399–410.
doi:10.1017/S0031182006000540 Printed in the United Kingdom

from serum is essential for survival of the intra-erythrocytic *Plasmodium* parasite (Holz, 1977; Vial and Ancelin, 1998; Mitamura and Palacpac, 2003). Moreover, a recent report shows that the intra-erythrocytic *P. falciparum* has no or little capacity to elongate or desaturate fatty acids (Krishnegowda and Gowda, 2003). These features of fatty acid metabolism in *P. falciparum* stand in contrast with those in a majority of organisms, wherein both *de novo* lipid biosynthesis and modification (elongation and desaturation) are important for homeostasis.

In this study, we screened combinations of 3 fatty acids (saturated and unsaturated) to determine which of them can sustain the long-term culture of *P. falciparum in vitro*. We also used metabolic labelling and gas chromatography (GC) to determine how serum-derived fatty acids essential for growth are metabolized by the parasite.

MATERIALS AND METHODS

Materials

Fatty acid-free BSA (used as lipid-free BSA) (Mitamura *et al.* 2000), various fatty acid species, and $C_{20:3,\ n-9}$ and $C_{22:6,\ n-3}$ methyl esters were purchased from Sigma-Aldrich. The $C_{18:1,\ n-7}$ methyl ester was from Supelco. Other fatty acid methyl esters (FAMEs) were from Matreya. Stock solutions of fatty acids (30 mM) and FAMEs (100 mM) were dissolved in ethanol and acetone, respectively, and stored at −20 °C until use. [1-^{14}C]-oleic acid (51 mCi mmol^{-1}) was from Amersham Biosciences Corp. [1-^{14}C]-palmitic acid (60 mCi mmol^{-1}) was from NEN Life Science Products. [1-^{14}C]-myristic acid (55 mCi mmol^{-1}), [1-^{14}C]-stearic acid (55 mCi mmol^{-1}), and [1-^{14}C]-linoleic acid (50 mCi mmol^{-1}) were from American Radiolabeled Chemicals Inc. Silica gel 60 high-performance TLC and silanized silica gel 60 TLC plates were from Merck.

Parasite culture

Culture of the *P. falciparum* Honduras-1 line and the growth-promoting activity assay were performed essentially as described previously (Mitamura *et al.* 2000; Hanada *et al.* 2000) with slight modification. If the parasitaemia at 96 h was above 0·1%, the culture was diluted to 0·1% and incubated for another 96 h. The growth-promoting activities were assessed at 96 h and 192 h. The media used were as described previously (Palacpac *et al.* 2004).

Gas chromatography analysis of fatty acid

Total lipids of pooled human serum from 10 individuals were extracted by Bligh and Dyer's method (Bligh and Dyer, 1959). Fatty acids were purified from the obtained total lipids using an NH_2 Sep-Pak plus column (Waters) as described previously (Kaluzny *et al.* 1985). The fatty acids collected were transmethylated in 1 ml of 5% methanolic HCl at 80 °C for 2 h (Khunyoshyeng *et al.* 2002). The resulting FAMEs were extracted twice with 1·5 ml of *n*-hexane, dried with a Speed Vac concentrator, and stored at 4 °C until use. Prior to analysis, the FAMEs were dissolved in 140 μl of acetone, and a 2 μl sample was automatically injected into a GC353B gas chromatograph (GL sciences) equipped with a TC-FFAP capillary column (0·25 mm × 30 m; df = 0·25 μm) and a flame ionization detector (GL sciences). The column pressure was set at 1·1 kg/cm^2, the split mode was set at a ratio of 50 : 1, and the programme to control the oven temperature was as follows: 45 °C for 3 min, followed by an increase from 45 °C to 230 °C at 10 °C/min, and, finally, maintenance at 230 °C for 40 min.

Total lipids were extracted from *P. falciparum*-infected erythrocytes enriched using Percol from cultures as described previously (Palacpac *et al.* 2004). The obtained lipids were dissolved in 1·8 ml of 10% KOH in 66% methanol and saponified at 65 °C for 60 min (Matsuzaka *et al.* 2002). After acidification with 1 ml of ice-cold 6 M HCl, the fatty acids liberated were extracted by Bligh and Dyer's method (Bligh and Dyer, 1959). The collected fatty acids were transmethylated, and the resulting FAMEs were analysed as described above. To determine the background of the erythrocyte fatty acid content, the same number of uninfected erythrocytes incubated in various media used for parasite cultures were similarly treated and analysed. In all the infected erythrocytes samples, more than 90% are schizont stage.

At least 4 injections per sample were performed, and the average of the results obtained from 3 independent chromatograms was used for quantification. The concentration of each fatty acid species detected in the sample was estimated from the peak area using standard curves for various control FAMEs as determined from the analyses of 4 different concentrations of each control FAME (the linear regression coefficients of the standard curves were >0·999). Changes in the fatty acid content due to parasitic infection were determined by subtracting the results for uninfected erythrocytes from those for *P. falciparum*-infected erythrocytes. In all cases, the results for infected erythrocytes refer to the changes from uninfected erythrocytes. Also, the amounts of fatty acids in the uninfected erythrocytes were less than 4% of those in infected erythrocytes. All results were normalized by the amount of fatty acid in 10^7 infected erythrocytes as determined by measurement of the parasitaemia in Percol-enriched samples.

Metabolic labelling

Tightly synchronized cultures of Honduras-1 line *P. falciparum*, which have a 5 h life-span, were

Table 1. Fatty acid content in pooled human serum and *Plasmodium falciparum*-infected erythrocytes

(The samples were prepared from the pooled human serum from 10 individuals and the culture maintained in standard medium supplemented with this serum. Data for the pooled human serum and the parasitized erythrocytes are expressed as μM and nmole per 10^7 infected erythrocytes, respectively.)

	14:0	16:0	16:1*n*-7	18:0	18:1*n*-9	18:1*n*-7	18:2*n*-6	18:3*n*-3	20:4*n*-6	22:6*n*-6
Pooled human serum	0·29	7·78	0·51	2·83	6·95	0·44	3·56	0·26	0·72	0·79
Parasitized erythrocyte	0·84	19·01	0·73	2·18	12·24	0·55	8·62	0·50	1·00	0·22

metabolically labelled either in standard or serum-free medium with ^{14}C-labelled fatty acids, and total lipids were extracted and analysed as described previously (Palacpac *et al.* 2004) except that a silica gel 60 high-performance TLC plate was used. In experiments performed in standard medium, cultures contained the pooled human serum from 10 individuals (for which the fatty acid content was determined by GC) mixed with one of the following ^{14}C-labelled fatty acids at a final specific activity of 8·3 mCi mmole^{-1}: [1-^{14}C]-myristic acid ($C_{14:0}$), [1-^{14}C]-palmitic acid ($C_{16:0}$), [1-^{14}C]-stearic acid ($C_{18:0}$), [1-^{14}C]-oleic acid ($C_{18:1,\ n\text{-}9}$), and [1-^{14}C]-linoleic acid ($C_{18:2,\ n\text{-}6}$). The purity of these radio-isotope labelled fatty acids was confirmed by TLC on a silanized plate in 70 : 50 : 35 : 1 (v/v/v/v) acetone/ methanol/ water/acetic acid prior to use. In experiments performed in serum-free medium, cultures were treated with 60 μM reconstituted lipid-associated BSA containing combinations of 3 fatty acids that supported parasite growth for at least 7 subcultures along with the appropriate ^{14}C-labelled fatty acids. In both standard and serum-free media, parasite development and appearance were monitored by microscopical observation of Giemsa-stained thin smears.

To identify the fatty acid species produced by parasite-associated elongase and desaturase activities, fatty acids were liberated from the total lipids extracted from metabolically labelled erythrocytes and then derivatized to methyl esters as described above for GC analysis. The obtained products were separated by TLC on a silanized plate in 70 : 50 : 35 : 1 (v/v/v/v) acetone/methanol/ water/acetic acid and analysed using an image analyser (Fuji Photo Film Co.) as described previously (Palacpac *et al.* 2004).

RESULTS

Comprehensive analysis of the combinations of three human serum-derived fatty acids for the intraerythrocytic proliferation of P. falciparum

To establish the baseline fatty acid composition of human serum, we used GC to analyse the average fatty acid composition of human serum pooled from 10 individuals. We identified 8 fatty acid species ($C_{16:0}$, $C_{18:1,\ n\text{-}9}$, $C_{18:2,\ n\text{-}6}$, $C_{18:0}$, $C_{22:6,\ n\text{-}6}$, $C_{20:4,\ n\text{-}6}$, $C_{16:1,\ n\text{-}7}$, and $C_{18:1,\ n\text{-}7}$) that each accounted for more than 1·5% of the total amount of fatty acid. Their estimated concentrations were 7·78, 6·95, 3·55, 2·83, 0·79, 0·72, 0·51, and 0·44 μM, respectively (Table 1).

We next examined the effect of these 8 fatty acids together with the $C_{14:0}$, which is the final product of *de novo* fatty acid synthesis in *P. falciparum* (Surolia and Surolia, 2001), and $C_{18:3,\ n\text{-}3}$, an essential fatty acid species in humans, on the intraerythrocytic proliferation of *P. falciparum*. We first determined the growth rates at 96 h and 192 h in a serum-free medium supplemented with reconstituted lipid-associated BSAs containing combinations of 3 fatty acids. All of the fatty acids identified were examined

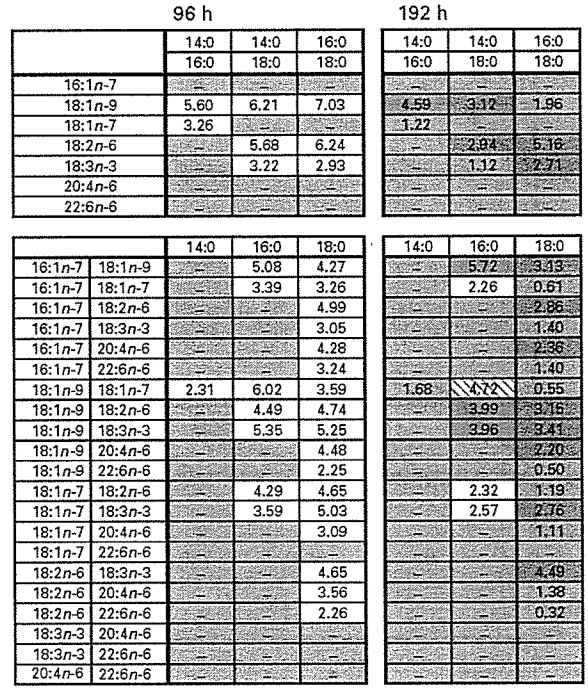

Fig. 1. Parasite growth rates in serum-free medium supplemented with reconstituted lipid-associated BSA containing a combination of saturated and unsaturated fatty acids. The combinations giving growth rates less than 2 are coloured grey; those containing $C_{18:0}$ are shown in red; those containing both $C_{16:0}$ and $C_{18:1,\ n\text{-}9}$ are in green; and those containing both $C_{16:0}$ and $C_{18:1,\ n\text{-}7}$ are in yellow. The growth rates in standard and in serum-free medium supplemented with reconstituted lipid-associated BSA containing $C_{16:0}/C_{18:1,\ n\text{-}9}$ were 8·14 and 6·07, respectively.

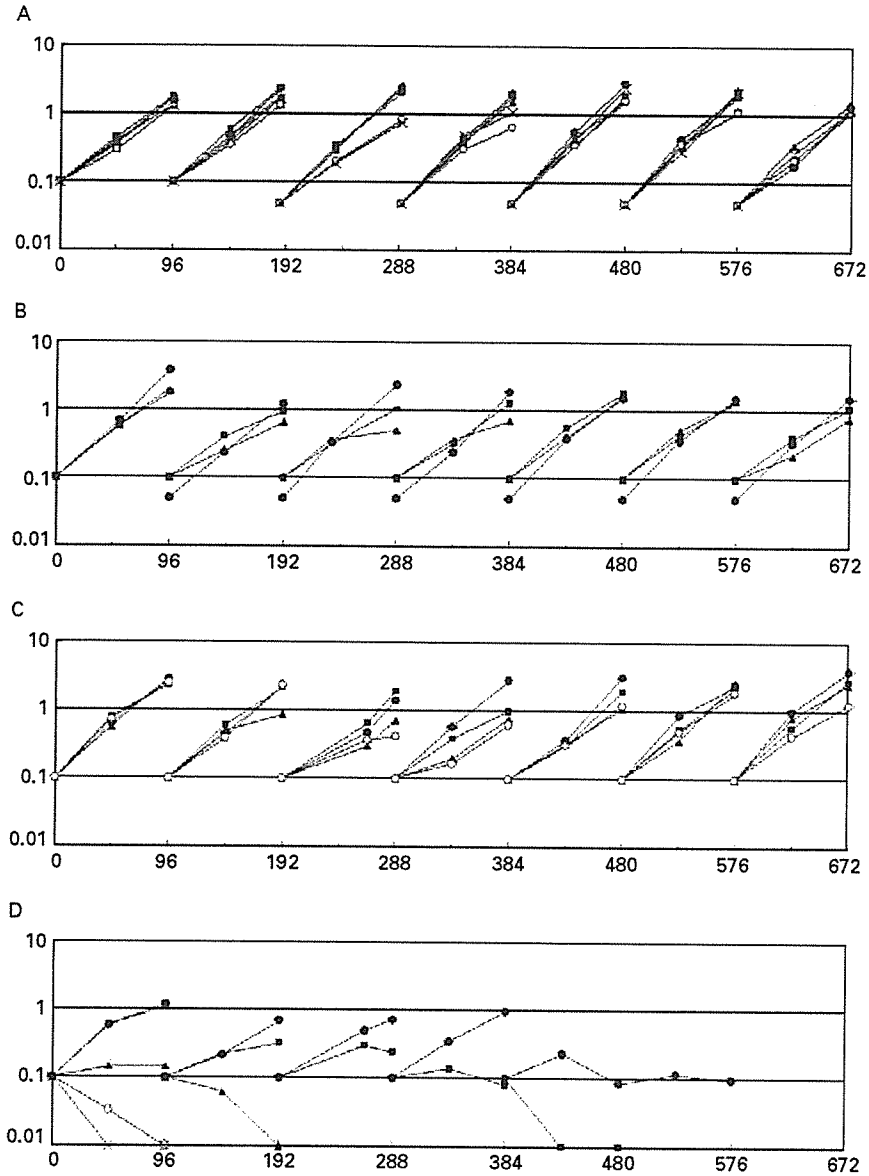

Fig. 2. The growth profile of the parasites in serum-free medium supplemented with reconstituted lipid-associated BSA containing a combination of fatty acids. (A) $C_{16:0}/C_{18:1,\ n\text{-}9}$ (●), $C_{16:0}/C_{18:1,\ n\text{-}9}/C_{14:0}$ (■), $C_{16:0}/C_{18:1,\ n\text{-}9}/C_{16:1,\ n\text{-}7}$ (▲), $C_{16:0}/C_{18:1,\ n\text{-}9}/C_{18:2,\ n\text{-}6}$ (○), and $C_{16:0}/C_{18:1,\ n\text{-}9}/C_{18:3,\ n\text{-}3}$ (×). (B) $C_{16:0}/C_{18:1,\ n\text{-}9}/C_{18:1,\ n\text{-}7}$ (●), $C_{16:0}/C_{18:1,\ n\text{-}7}/C_{18:2,\ n\text{-}6}$ (■), and $C_{16:0}/C_{18:1,\ n\text{-}7}/C_{18:3,\ n\text{-}3}$ (▲). (C) $C_{16:0}/C_{18:0}/C_{18:2,\ n\text{-}6}$ (●), $C_{14:0}/C_{18:0}/C_{18:2,\ n\text{-}6}$ (■), $C_{14:0}/C_{18:0}/C_{18:1,\ n\text{-}9}$ (▲), and $C_{18:0}/C_{18:1,\ n\text{-}9}/C_{18:2,\ n\text{-}6}$ (○). (D) $C_{18:0}/C_{16:1,\ n\text{-}7}/C_{18:1,\ n\text{-}9}$ (●), $C_{18:0}/C_{18:2,\ n\text{-}6}/C_{20:4,\ n\text{-}6}$ (■), $C_{16:0}/C_{18:1,\ n\text{-}9}/C_{20:4,\ n\text{-}6}$ (▲), $C_{14:0}/C_{16:1,\ n\text{-}7}/C_{18:2,\ n\text{-}6}$ (○), and $C_{14:0}/C_{18:2,\ n\text{-}6}/C_{20:4,\ n\text{-}6}$ (×). X- and Y-axes indicate parasitaemia (%) and period (h) of the parasite cultures, respectively.

with the exception of completely saturated or unsaturated species because they are expected to be detrimental for parasite growth (Mitamura *et al.* 2000). Of the total of 84 combinations, 20 supported parasite growth for at least 192 h. Overall, the growth rates were significantly affected by changing only 1 fatty acid (Fig. 1).

We next examined whether these 20 combinations could sustain the continuous culture of *P. falciparum*. We found 11 combinations (Fig. 2A–C) that could maintain the exponential growth of the parasite during the course of continuous culture for at least 28 days (equivalent to 7 subcultures), whereas the remaining 9 combinations caused a gradual decrease in the growth rates until the parasites finally disappeared (Fig. 2D; data not shown). These results indicate that particular combinations of saturated and unsaturated fatty acids are needed to sustain long-term intraerythrocytic proliferation of *P. falciparum* and that chain length, extent of unsaturation,

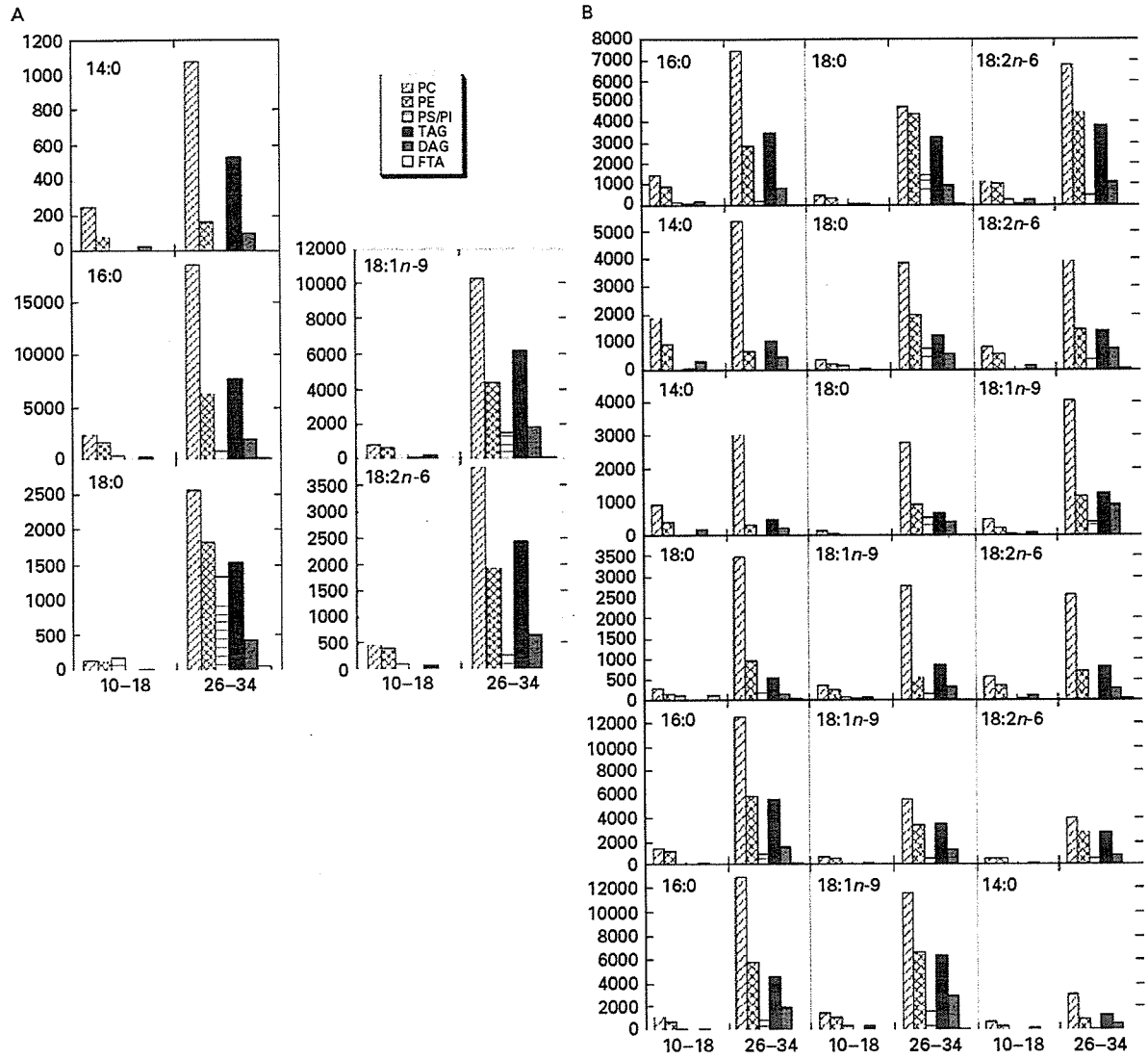

Fig. 3. Comparison of the profiles of the lipid species generated by metabolism of different fatty acids in standard and in a serum-free medium supplemented with reconstituted lipid-associated BSA containing the combinations of 3 fatty acids. (A) Standard medium. (B) Serum-free medium. Each row represents a combination of fatty acids added to the serum-free medium. The specific ^{14}C-labelled fatty acids used for metabolic labelling are indicated in each graph. The amount of each lipid is quantified by densitometry analysis using an image analyser (Fuji Photo Film Co.) and is expressed as arbitrary units.

and position of double bonds are critical parameters regulating the growth.

Comparison of the profiles of the lipid species metabolized from different fatty acids in standard and serum-free media

Six combinations of fatty acids ($C_{14:0}/C_{16:0}/C_{18:1,\ n\text{-}9}$, $C_{14:0}/C_{18:0}/C_{18:1,\ n\text{-}9}$, $C_{14:0}/C_{18:0}/C_{18:2,\ n\text{-}6}$, $C_{16:0}/C_{18:1,\ n\text{-}9}/C_{18:2,\ n\text{-}6}$, $C_{16:0}/C_{18:0}/C_{18:2,\ n\text{-}6}$, and $C_{18:0}/C_{18:1,\ n\text{-}9}/C_{18:2,\ n\text{-}6}$) were able to maintain the *P. falciparum* subculture for over 6 months (data not shown), suggesting that, like human serum, these combinations can support parasite culture indefinitely. We next used metabolic labelling with ^{14}C-fatty acids to examine the lipid profiles generated from these 5 fatty acids in standard and a serum-free media. All of the fatty acids tested could be metabolized into phosphatidylcholine, phosphatidylethanolamine, phosphatidylserine, phosphatidylinositol, diacylglycerol, and triacylglycerol. Further, the level of each lipid species and the lipid profiles were similar at early (ring to early trophozoite; 10–18 h) and mature stages (mature trophozoite to schizont; 26–34 h) (Figs 3A, B and 4A–G). These results indicate that, despite the requirement of particular fatty acids for growth, intraerythrocytic *P. falciparum* can metabolize a broad range of serum-derived fatty acids.

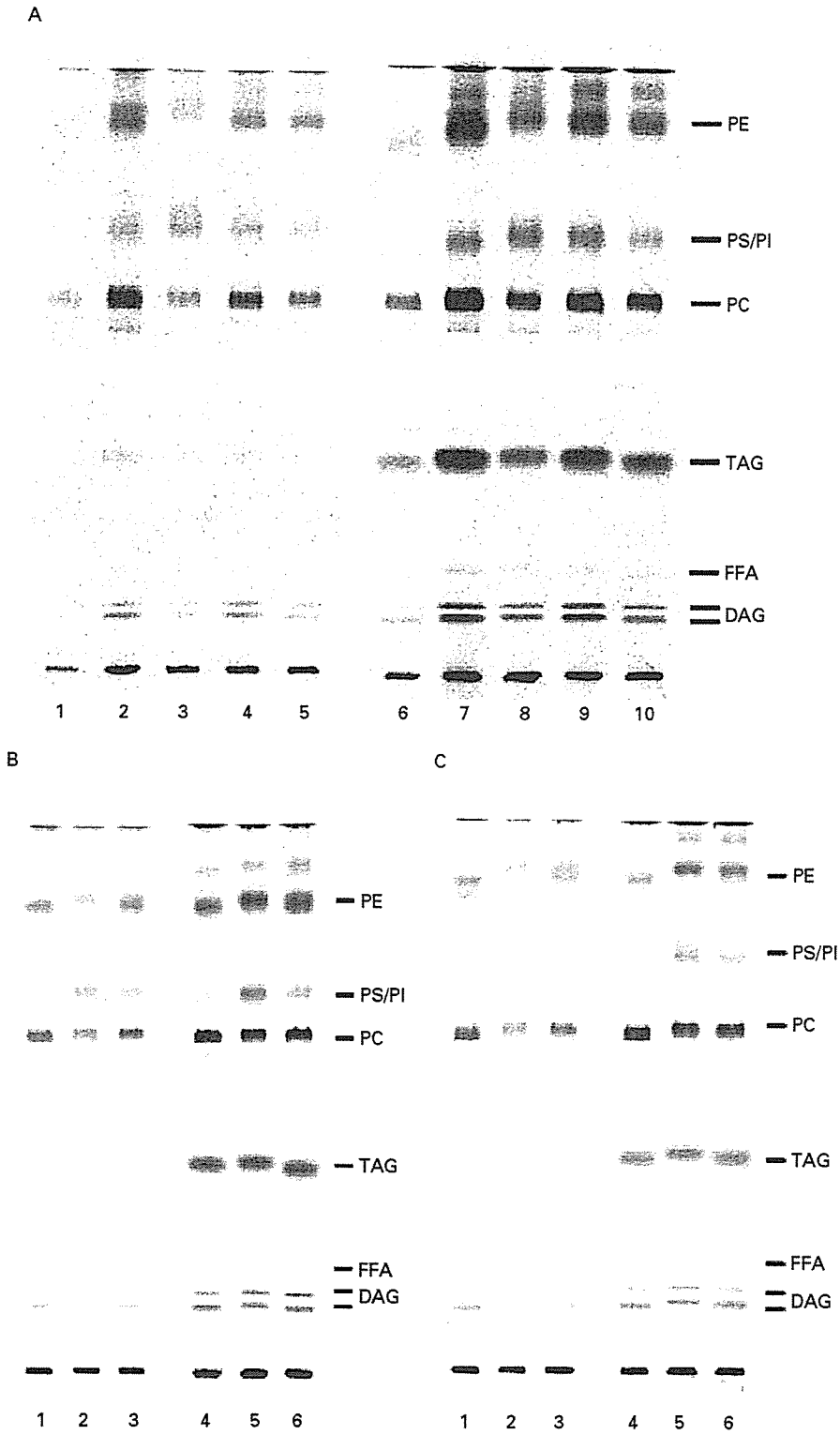

Fig. 4. Analysis of lipid species generated by metabolism from different fatty acids in standard medium or serum-free medium supplemented with reconstituted lipid-associated BSA containing combination of fatty acids. (A) Standard medium. High-performance TLC of the samples metabolically labelled from 10 to 18 h (lanes 1–5) and from 26 to 34 h (lanes 6–10) during intraerythrocytic development. The following ^{14}C-fatty acids were used for metabolic labelling: ^{14}C-$C_{14:0}$ (lanes 1 and 6), ^{14}C-$C_{16:0}$ (lanes 2 and 7), ^{14}C-$C_{18:0}$ (lanes 3 and 8), ^{14}C-$C_{18:1,\ n\text{-}9}$ (lanes 4 and 9), and ^{14}C-$C_{18:2,\ n\text{-}6}$ (lanes 5 and 10). (B-G) Serum-free media. The following combinations were added to the medium: $C_{16:0}$/$C_{18:0}$/$C_{18:2,\ n\text{-}6}$ (B), $C_{14:0}$/$C_{18:0}$/$C_{18:2,\ n\text{-}6}$ (C), $C_{14:0}$/$C_{18:0}$/$C_{18:1,\ n\text{-}9}$ (D), $C_{18:0}$/$C_{18:1,\ n\text{-}9}$/$C_{18:2,\ n\text{-}6}$ (E), $C_{16:0}$/$C_{18:1,\ n\text{-}9}$/$C_{18:2,\ n\text{-}6}$ (F), and $C_{16:0}$/$C_{18:1,\ n\text{-}9}$/$C_{14:0}$ (G). High-performance TLC of the samples metabolically labelled from

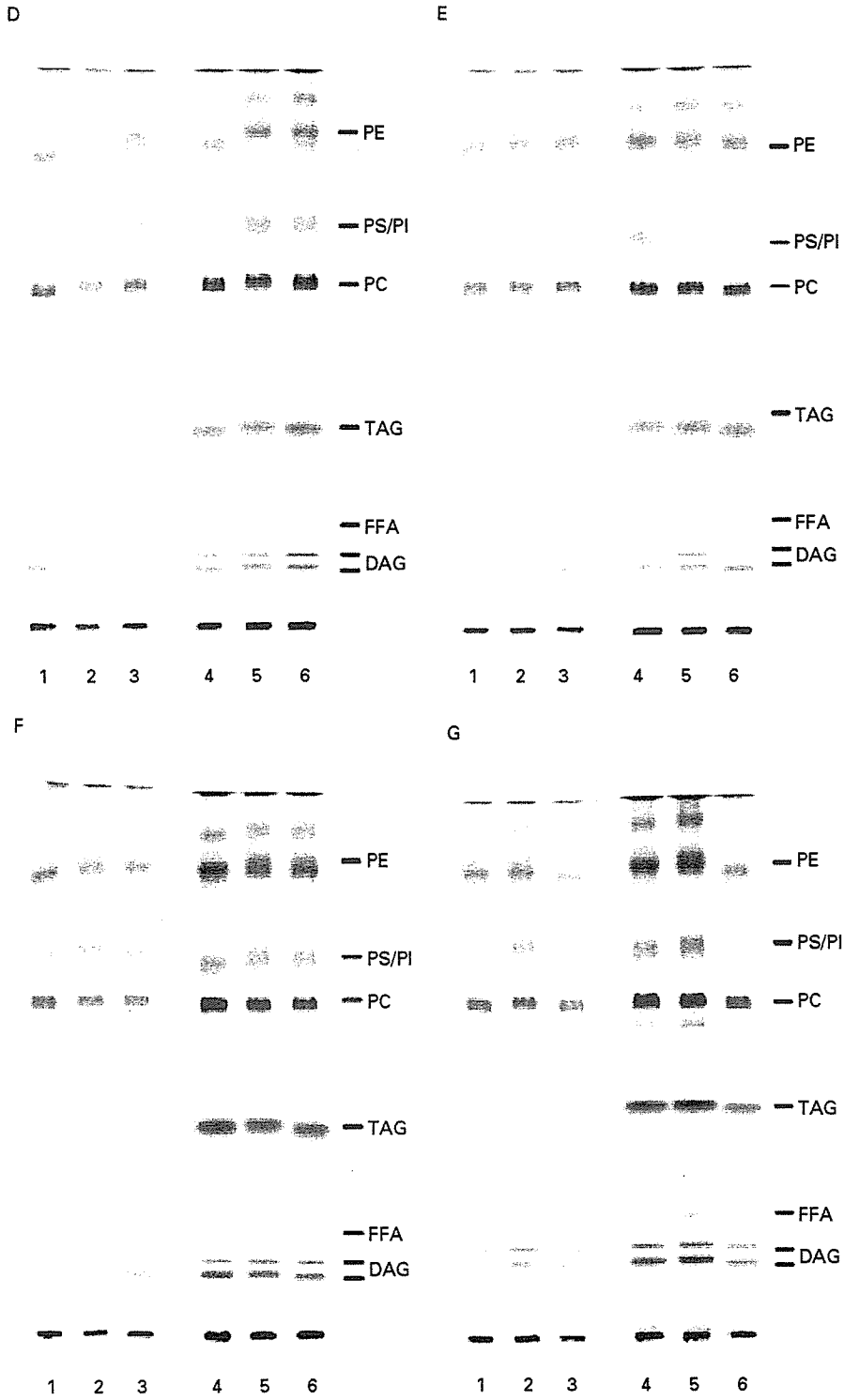

10 to 18 h (lanes 1–3) and from 26 to 34 h (lanes 4–6) during intraerythrocytic development. The following ^{14}C-fatty acids were used for metabolic labelling: (B) ^{14}C-$C_{16:0}$ (lanes 1 and 4), ^{14}C-$C_{18:0}$ (lanes 2 and 5), and ^{14}C-$C_{18:2,\ n-6}$ (lanes 3 and 6); (C) ^{14}C-$C_{14:0}$ (lanes 1 and 4), ^{14}C-$C_{18:0}$ (lanes 2 and 5), and ^{14}C-$C_{18:2,\ n-6}$ (lanes 3 and 6); (D) ^{14}C-$C_{14:0}$ (lanes 1 and 4), ^{14}C-$C_{18:0}$ (lanes 2 and 5), and ^{14}C-$C_{18:1,\ n-9}$ (lanes 3 and 6); (E) ^{14}C-$C_{18:0}$ (lanes 1 and 4), ^{14}C-$C_{18:1,\ n-9}$ (lanes 2 and 5), and ^{14}C-$C_{18:2,\ n-6}$ (lanes 3 and 6); (F) ^{14}C-$C_{16:0}$ (lanes 1 and 4), ^{14}C-$C_{18:1,\ n-9}$ (lanes 2 and 5), and ^{14}C-$C_{18:2,\ n-6}$ (lanes 3 and 6); and (G) ^{14}C-$C_{16:0}$ (lanes 1 and 4), ^{14}C-$C_{18:1,\ n-9}$ (lanes 2 and 5), and ^{14}C-$C_{14:0}$ (lanes 3 and 6). The polar and neutral lipids are shown in the upper and lower panels, respectively, and the positions of the standard lipids are indicated on the right side. PE, phosphatidylethanolamine; PS, phosphatidylserine; PI, phosphatidylinositol; PC, phosphatidylcholine; TAG, triacylglycerol; FFA, fatty acid; DAG, diacylglycerol.

Table 2. Summary of the parasite-associated capacities for fatty acid desaturation and elongation

(Data shown are the averages of the conversion rates obtained from 3 independent cultures for each GC and metabolic labelling analyses and are expressed as percentages ±S.D. The conversion rate is calculated by dividing the amount of the corresponding product by the total amount of the substrate and product, and multiplying by 100. The conversion rate in metabolic labelling is quantified also by densitometry using radio-isotope labelled fatty acids as a standard, e.g. 80·4 and 1·8 pmole per h per 10^7 infected erythrocytes for desaturating the *n*-9 position of $C_{18:0}$ of the $C_{16:0}/C_{18:0}/C_{18:2,\ n\text{-}6}$ sample and for elongating $C_{14:0}$ into $C_{16:0}$ of the $C_{14:0}/C_{18:0}/C_{18:2,\ n\text{-}6}$ sample, respectively. n.d., not done; n. a., not applicable.)

	16:0→16:1*n*-7		18:0→18:1*n*-9		14:0→16:0	16:0→18:0
	GC	Metabolic labelling	GC	Metabolic labelling	Metabolic labelling	Metabolic labelling
16:0/18:0/18:2*n*-6	0·6±0·0	0·5±0·1	36·1±2·8	31·2±1·1		0·0±0·0
14:0/18:0/18:2*n*-6			12·6±2·4	10·7±0·5	1·4±0·4	
14:0/18:0/18:1*n*-9			n.a.	24·6±0·6	1·6±0·4	
18:0/18:1*n*-9 /18:2*n*-6			n.a.	15·9±0·5		
14:0/16:0/18:1*n*-9	n.d.	1·2±0·1			0·8±0·3	0·0±0·0
16:0/18:1*n*-9/18:2*n*-6	n.d.	0·9±0·0				0·0±0·0
16:0/18:1 *n*-9	1·6±0·3	1·2±0·2				0·7±0·0
Human serum	n.a.	0·6±0·1	n.a.	29·4±0·1	0·0±0·0	0·0±0·0

Intraerythrocytic P. falciparum *can elongate and desaturate serum-derived fatty acids*

The fatty acids from the medium were mostly converted into the major lipid components of the parasite's membranes and lipid body (Figs 3A, B and 4A–G; Vial *et al.* 1982; Palacpac *et al.* 2004). To determine which fatty acid species were generated by metabolism, we analysed the metabolically labelled parasites by TLC. Analysis of the ^{14}C-$C_{18:0}$-labelled samples showed ^{14}C-labelled $C_{18:1}$ methyl ester was present in the infected erythrocytes but not in the uninfected erythrocytes (Fig. 5A). Even when the imaging plates for the uninfected erythrocyte samples were overexposed until the intensity of the $C_{18:0}$ signals reached the levels in the infected cells, a $C_{18:1}$ methyl ester signal could not be seen. A signal corresponding to ^{14}C-labelled $C_{16:1}$ methyl ester could also be specifically detected in the infected but not the uninfected ^{14}C-$C_{16:0}$-labelled erythrocytes. In contrast, we did not detect signals for fatty acids produced by Δ9-, Δ12-, or Δ15-desaturases from infected erythrocytes metabolically labelled with ^{14}C-$C_{14:0}$, ^{14}C-$C_{18:1,\ n\text{-}9}$, or ^{14}C-$C_{18:2,\ n\text{-}6}$ (data not shown). These results clearly indicate that the intraerythrocytic *P. falciparum* can desaturate mainly the *n*-9 position of $C_{16:0}$ and $C_{18:0}$ and that this activity is unaffected by the culture conditions (Table 2).

In contrast to the desaturase activity, the ability to elongate fatty acids taken up from the surroundings can be detected only under limited culture conditions. We were able to detect the production of $C_{18:0}$ from ^{14}C-$C_{16:0}$ when the parasites were cultured in serum-free medium supplemented with lipid-rich BSA containing $C_{16:0}/C_{18:1,\ n\text{-}9}$ (Fig. 5B) but not when they were cultured in standard or serum-free medium supplemented with lipid-rich BSA containing $C_{16:0}/C_{18:0}/C_{18:2,\ n\text{-}6}$, $C_{14:0}/C_{16:0}/C_{18:1,\ n\text{-}9}$, or $C_{16:0}/C_{18:1,\ n\text{-}9}/C_{18:2,\ n\text{-}6}$ (data not shown). No $C_{18:0}$ signals could be observed in uninfected erythrocytes even when the images were overexposed. Similarly, in the presence of ^{14}C-$C_{14:0}$, a small but significant production of $C_{16:0}$ was observed in parasites grown in serum-free medium supplemented with lipid-rich BSA containing $C_{14:0}/C_{16:0}/C_{18:1,\ n\text{-}9}$, $C_{14:0}/C_{18:0}/C_{18:1,\ n\text{-}9}$, or $C_{14:0}/C_{18:0}/C_{18:2,\ n\text{-}6}$ but not in standard medium (data not shown). These results suggest that the

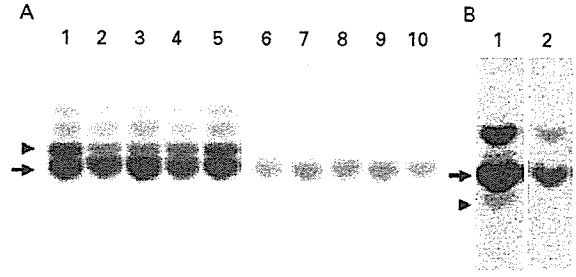

Fig. 5. Analysis of the parasite-associated capacities for desaturating and elongating serum-derived fatty acids. (A) Desaturation. Silanized TLC of FAMEs prepared from metabolically ^{14}C-$C_{18:0}$-labelled infected (lanes 1–5) and uninfected (lanes 6–10) erythrocytes. The fatty acid combinations used to supplement serum-free medium metabolic labelling were as follows: $C_{16:0}/C_{18:0}/C_{18:2,\ n\text{-}6}$ (lanes 1 and 6), $C_{14:0}/C_{18:0}/C_{18:2,\ n\text{-}6}$ (lanes 2 and 7), $C_{14:0}/C_{18:0}/C_{18:1,\ n\text{-}9}$ (lanes 3 and 8), and $C_{18:0}/C_{18:1,\ n\text{-}9}/C_{18:2,\ n\text{-}6}$ (lanes 4 and 9). Human serum (lanes 5 and 10) was also used for metabolic labelling. The arrowhead and arrow indicate the position of methyl ethers of $C_{18:1,\ n\text{-}9}$ and $C_{18:0}$, respectively. (B) Elongation. FAMEs prepared from metabolically ^{14}C-$C_{16:0}$-labelled infected (lane 1) and uninfected (lanes 2) erythrocytes. The pair of $C_{16:0}/C_{18:1,\ n\text{-}9}$ was used to supplement serum-free medium metabolic labelling. The arrowhead and arrow indicate the position of methyl ethers of $C_{18:0}$ and $C_{16:0}$, respectively.

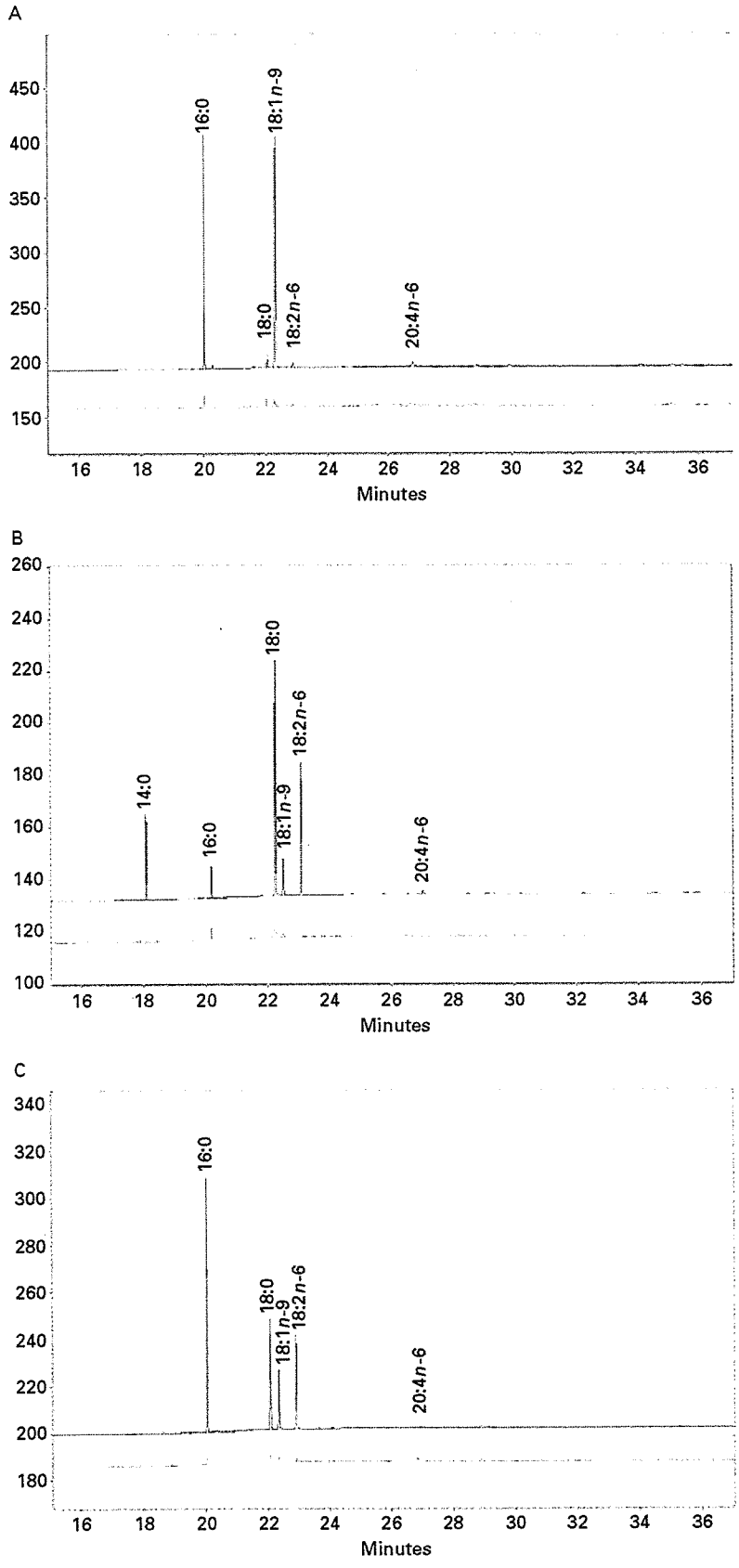

Fig. 6. GC analysis of the fatty acid composition and profile in *Plasmodium falciparum*-infected erythrocytes. Representative chromatograms from at least 4 injections are shown with black lines (infected erythrocytes) and grey lines (uninfected erythrocytes). The combinations of fatty acids used for the cultures were (A) $C_{16:0}/C_{18:1,\ n\text{-}9}$, (B) $C_{14:0}/C_{18:0}/C_{18:2,\ n\text{-}6}$, and (C) $C_{16:0}/C_{18:0}/C_{18:2,\ n\text{-}6}$.

Table 3. Fatty acid content in *Plasmodium falciparum*-infected erythrocyte

(The samples were prepared from the cultures maintained in serum-free medium supplemented with reconstituted lipid-associated BSA containing a combination of fatty acids. Data shown are the averages of the results obtained from three independent cultures and are expressed as nmole per 10^7 infected erythrocytes ±S.D.)

	14:0	16:0	16:1*n*-7	18:0	18:1*n*-9	18:1*n*-7	18:2*n*-6	18:3*n*-3	20:4*n*-6	22:6*n*-6
16:0/18:1*n*-9	0·05±0·03	22·51±1·79	0·36±0·03	0·16±0·23	28·03±1·42	0	0·31±0·01	0	0·37±0·21	0
14:0/18:0/18:2*n*-6	10·08±7·61	1·75±0·15	0	19·37±1·50	2·80±0·62	0	11·66±2·28	0	0·18±0·23	0
16:0/18:0/18:2*n*-6	0·06±0·06	24·31±5·25	0·16±0·04	9·89±1·45	5·58±0·87	0	9·05±5·98	0	0·14±0·24	0

intraerythrocytic *P. falciparum* can elongate $C_{14:0}$ and $C_{16:0}$ into $C_{16:0}$ and $C_{18:0}$, respectively, and that this ability is regulated by the fatty acids available in their surroundings (Table 2).

Effect of the fatty acid composition in the medium on the fatty acid content of intraerythrocytic P. falciparum

We next used GC to examine the effects of the fatty acid composition of the surroundings on that of the parasites. In standard medium, the fatty acid species in the infected erythrocytes and the pooled human serum were similar (Table 1). The fatty acid composition in the infected erythrocytes is similar to that of parasites overall lipids described in the previous study (Hsiao *et al.* 1991). Likewise, in serum-free medium supplemented with reconstituted lipid-associated BSA containing $C_{16:0}$/ $C_{18:1}$, *n*-9, $C_{14:0}$/ $C_{18:0}$/$C_{18:2}$, *n*-6, or $C_{16:0}$/$C_{18:0}$/$C_{18:2}$, *n*-6, the fatty acid composition of the infected erythrocytes largely reflected the supplements (Fig. 6A–C and Table 3). These results confirm metabolic labelling results, namely, that intraerythrocytic *P. falciparum* can utilize a broad range of fatty acids from their surroundings for growth, suggesting that the majority of plasmodial factors involved in uptake/trafficking and metabolism of serum-derived fatty acids have broad specificity.

The results of GC analyses also support the idea that intraerythrocytic *P. falciparum* can carry out Δ9-desaturation. In serum-free media supplemented with reconstituted lipid-associated BSA containing $C_{14:0}$/$C_{18:0}$/$C_{18:2}$, *n*-6 or $C_{16:0}$/$C_{18:0}$/$C_{18:2}$, *n*-6, we detected a significant amount of $C_{18:1}$, *n*-9, which was not supplied in the medium (Fig. 6B, C and Table 3). GC analyses also indicated the presence of elongase activity in intraerythrocytic *P. falciparum*, although it was difficult to quantify due to a high background level of $C_{16:0}$ and $C_{18:0}$ in uninfected erythrocytes (Fig. 6A, B; data not shown).

DISCUSSION

Scavenging of fatty acids from serum is thought to be necessary for the growth of *P. falciparum* (Holz, 1977; Vial and Ancelin, 1998; Mitamura and Palacpac, 2003), and accumulating evidence suggests that these parasites possess unique metabolic pathways (Surolia and Surolia, 2001; Krishnegowda and Gowda, 2003). Therefore, determination of the human serum-derived fatty acid species essential for intraerythrocytic proliferation of *P. falciparum* and characterization of their metabolism is important in developing new strategy for controlling malaria. Here, we comprehensively analysed the effects of fatty acids present in human serum on the growth of *P. falciparum*. We found that particular combinations of three fatty acids support the continuous

culture of *P. falciparum* in serum-free medium. Metabolic labelling and GC analyses revealed that the fatty acids essential for parasite growth were metabolized similarly in media supplemented with human serum or with lipid-rich BSA containing the fatty acids. These studies also showed that the fatty acid composition of the infected erythrocytes largely reflect that of the growth medium. These two independent biochemical analyses suggest that the parasite can desaturate and elongate serum-derived fatty acids to a limited extent. These results imply that intraerythrocytic *P. falciparum* utilizes serum-derived fatty acids with little modification to form membranes and the lipid body. Furthermore, the results suggest that, in the parasite, *de novo* fatty acid synthesis makes a very limited contribution to acyl groups for lipid metabolism. These features of fatty acid metabolism in *P. falciparum* are unique because cells usually control their fatty acid composition by coordinating *de novo* biosynthesis, scavenging, and modification (e.g., desaturation and elongation).

Among 84 combinations of saturated and unsaturated fatty acids present in human serum, only 11 ($C_{14:0}/C_{16:0}/C_{18:1,\ n\text{-}9}$, $C_{14:0}/C_{18:0}/C_{18:1,\ n\text{-}9}$, $C_{14:0}/C_{18:0}/C_{18:2,\ n\text{-}6}$, $C_{16:0}/C_{16:1,\ n\text{-}7}/C_{18:1,\ n\text{-}9}$, $C_{16:0}/C_{18:1,\ n\text{-}9}/C_{18:1,\ n\text{-}7}$, $C_{16:0}/C_{18:1,\ n\text{-}9}/C_{18:2,\ n\text{-}6}$, $C_{16:0}/C_{18:1,\ n\text{-}9}/C_{18:3,\ n\text{-}3}$, $C_{16:0}/C_{18:1,\ n\text{-}7}/C_{18:2,\ n\text{-}6}$, $C_{16:0}/C_{18:1,\ n\text{-}7}/C_{18:3,\ n\text{-}3}$, $C_{16:0}/C_{18:0}/C_{18:2,\ n\text{-}6}$, and $C_{18:0}/C_{18:1,\ n\text{-}9}/C_{18:2,\ n\text{-}6}$) could sustain long-term *in vitro* culture of *P. falciparum* in serum-free medium. There was not a single specific fatty acid species included in all of the combinations, but there was a trend for a combination of $C_{16:0}$ and either $C_{18:1,\ n\text{-}9}$ or $C_{18:1,\ n\text{-}7}$, and $C_{18:0}$. Because $C_{16:0}$, $C_{18:1,\ n\text{-}9}$, and $C_{18:0}$ can be generated by *de novo* biosynthesis in humans, it is interesting to speculate that *P. falciparum* evolved to adapt to human hosts in which the other fatty acids vary according to diet and health.

The *P. falciparum* genome contains candidate orthologues of a Δ-9 desaturases (gene ID in Plasmo DB (http://v5-0.plasmodb.org/plasmo-release5-0/home.jsp): PFE0555w) and elongases (gene IDs in PlasmoDB (http://v5-0.plasmodb.org/plasmo-release5-0/home.jsp): PFA0455c, PFF0290w, and PFI0980w). In agreement with this, our results suggest that intraerythrocytic *P. falciparum* can desaturate and elongate fatty acids taken up from their surroundings. Our results, however, do not agree with a previous report that the parasite has little or no ability to elongate or otherwise modify fatty acids scavenged from the external medium (Krishnegowda and Gowda, 2003). This discrepancy could be due to differences in the culture conditions.

Metabolic labelling and GC analyses also revealed that the parasite can produce $C_{16:1,\ n\text{-}7}$ and $C_{18:1,\ n\text{-}9}$ from $C_{16:0}$ and $C_{18:0}$, respectively. Because only one candidate gene for a putative *P. falciparum* desaturase could be found in its genome, it is likely that both $C_{16:1,\ n\text{-}7}$ and $C_{18:1,\ n\text{-}9}$ are produced by a single desaturase, although different levels may be generated due to substrate specificity of the plasmodial enzyme. Further, our results suggest that the capacity to desaturate $C_{18:0}$ into $C_{18:1,\ n\text{-}9}$ in the intraerythrocytic parasite is not affected by the culture conditions. From this, we infer that $C_{18:1,\ n\text{-}9}$ is always present in the parasites regardless of the environmental conditions and that it is therefore necessary for intraerythrocytic proliferation.

We thank Drs Toshihiro Horii and Nirianne Marie Q. Palacpac for discussion and Ms. Hisako Araki, Ms. Kumiko Tai, and Mr. Takenori Taniguchi for technical assistance. This work was supported by grants (to T.M.) from the PRESTO program of the Japan Science and Technology Agency and from the Pharmaceutical and Medical Devices Agency as well as a Grant-in-Aid for scientific research on priority areas (to K.K.) from the Japanese Ministry of Education, Science, Culture, and Sports (13226015, 13854011 and 1720913).

REFERENCES

Asahi, H., Kanazawa, T., Hirayama, N. and Kajihara, Y. (2005). Investigating serum factors promoting erythrocytic growth of *Plasmodium falciparum*. *Experimental Parasitology* **109**, 7–15.

Bligh, E. G. and Dyer, W. J. (1959). A rapid method of total lipid extraction and purification. *Canadian Journal of Biochemistry and Physiology* **37**, 911–917.

Grellier, P., Rigomier, D., Clavey, V., Fruchart, J.-C. and Schrevel, J. (1991). Lipid traffic between high density proteins and *Plasmodium falciparum*-infected red blood cells. *Journal of Cell Biology* **112**, 267–277.

Hanada, K., Mitamura, T., Fukasawa, M., Magistrado, P. A., Horii, T. and Nishijima, M. (2000). Neutral sphingomyelinase activity dependent on Mg^{2+} and anionic phospholipids in the intraerythrocytic malaria parasite *Plasmodium falciparum*. *The Biochemical Journal* **346**, 671–677.

Heusser, D. (1968). Thin-layer chromatography of fatty acids on silanized silica gel. *Journal of Chromatography* **33**, 62–69.

Holz, G. G. (1977). Lipids and the malaria parasite. *Bulletin of the World Health Organization* **55**, 237–248.

Hsiao, L. L., Howard, R. J., Aikawa, M. and Taraschi, T. F. (1991). Modification of host cell membrane lipid composition by the intra-erythrocytic human malaria parasite *Plasmodium falciparum*. *The Biochemical Journal* **274**, 121–132.

Kaluzny, M. A., Duncan, L. A., Merritt, M. V. and Epps, D. E. (1985). Rapid separation of lipid classes in high yield and purity using bonded phase columns. *Journal of Lipid Research* **26**, 135–140.

Khunyoshyeng, S., Cheevadhanarak, S., Rachdawong, S. and Tanticharoen, M. (2002). Differential expression of desaturases and changes in fatty acid composition during sporangiospore germination and development in *Mucor rouxii*. *Fungal Genetics and Biology* **37**, 13–21.

Krishnegowda, G. and Gowda, D. C. (2003). Intraerythrocytic *Plasmodium falciparum* incorporates extraneous fatty acids to its lipids without any structural

modification. *Molecular and Biochemical Parasitology* **132**, 55–58.

Matsuzaka, T., Shimano, H., Yahagi, N., Yoshikawa, T., Amemiya-Kudo, M., Hasty, A. H., Okazaki, H., Tamura, Y., Iizuka, Y., Ohashi, K., Osuga, J., Takahashi, A., Yato, S., Sone, H., Ishibashi, S. and Yamada, N. (2002). Cloning and characterization of a mammalian fatty acyl-CoA elongase as a lipogenic enzyme regulated by SREBPs. *Journal of Lipid Research* **43**, 911–920.

Mitamura, T., Hanada, K., Ko-Mitamura, E. P., Nishijima, M. and Horii, T. (2000). Serum factors governing intraerythrocytic development and cell cycle progression of *Plasmodium falciparum*. *Parasitology International* **49**, 219–229.

Mitamura, T. and Palacpac, N. M. Q. (2003). Lipid metabolism in *Plasmodium falciparum*-infected erythrocyte: possible new targets for malaria chemotherapy. *Microbes and Infections* **5**, 545–552.

Ofulla, A. V. O., Okaoye, V. C. N., Khan, B., Githure, J. I., Roberts, C. R., Johnson, A. J. and Martin, S. K. (1993). Cultivation of *Plasmodium falciparum* parasites in a serum-free medium. *American Journal of Tropical Medicine and Hygiene* **49**, 335–340.

Palacpac, N. M. Q., Hiramine, Y., Mi-ichi, F., Torii, M., Kita, K., Hiramatsu, R., Horii, T. and Mitamura, T. (2004). Developmental stage-specific triacylglycerol biosynthesis, degradation and trafficking as lipid bodies in *Plasmodium falciparum*-infected erythrocyte. *Journal of Cell Science* **117**, 1469–1480.

Surolia, N. and Surolia, A. (2001). Triclosan offers protection against blood stages of malaria by inhibiting enoyl-ACP reductase of *Plasmodium falciparum*. *Nature, Medicine* **7**, 167–173.

Trager, W. and Jensen, J. B. (1976). Human malaria parasites in continuous culture. *Science* **193**, 673–675.

Vial, H. J. and Ancelin, M. L. (1998). Malarial lipids. In *Parasite Biology, Pathogenesis, and Protection* (ed. Sherman, I. W.), pp. 159–175. ASM Press, Washington, D.C.

Vial, H. J., Thuet, M. J. and Philippot, J. R. (1982). Phospholipid biosynthesis in synchronous *Plasmodium falciparum* cultures. *Journal of Protozoology* **29**, 258–263.